NASA CONTRACTOR REPORT

NASA CR-1
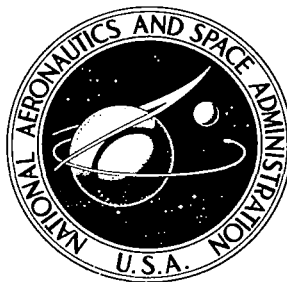
C.1

LARGE LOW-FREQUENCY ORBITING RADIO TELESCOPE

by Hans U. Schuerch and John M. Hedgepeth

Prepared by
ASTRO RESEARCH CORPORATION
Santa Barbara, Calif.
for Goddard Space Flight Center

NATIONAL AERONAUTICS AND SPACE ADMINISTRATION • WASHINGTON, D. C. • OCTOBER 1968

NASA CR-1201

LARGE LOW-FREQUENCY ORBITING RADIO TELESCOPE

By Hans U. Schuerch and John M. Hedgepeth

Issued by Originator as Report No. ARC-R-282

NATIONAL AERONAUTICS AND SPACE ADMINISTRATION

FOREWORD

Since November 1965, Astro Research Corporation has been conducting studies of the feasibility of a large (1500-meter) orbiting radio telescope under Contract NAS7-426 for National Aeronautics and Space Administration.

Mr. Robert Drummond is the NASA Goddard Space Flight Center Project Study Manager, and Mr. John Gates is the Technical Officer. Dr. John M. Hedgepeth is the Astro Research Corporation program director.

SUMMARY

Studies have been performed of the feasibility of a large (1500-meter) orbiting paraboloidal antenna for use in low-frequency (< 10 MHz) radio astronomy. Such a radio telescope would be extremely useful in a variety of scientific astronomical studies.

A conceptual configuration has been evolved which consists of a tenuous conductive paraboloidal network which is deployed and stiffened by centrifugal forces due to spin about the axis of symmetry.

Meridional tension forces are produced in the net by means of an extremely long deployable mast which runs along the axis of symmetry and forms the backbone of the structure. The entire configuration is deployed from a package suitable for launch on such vehicles as the Titan III.

Results of the various theoretical and experimental analyses which have led to this baseline concept are summarized. A current subscale ground-test program is described, and indications are given of the desirability for flight tests to develop technology and establish feasibility.

TABLE OF CONTENTS

LIST OF FIGURES

INTRODUCTION

In its report of February 1967, the President's Science Advisory Committee recommended that "...the government adopt as a primary goal in the application of space technology for scientific purposes a program leading to the establishment in earth orbit of a number of astronomical observatories capable of:

(1) exploring the full range of the spectrum not accessible from the ground...,

(2) scientific control directly by astronomers on earth, and,

(3) extended useful life through intermittent maintenance and modernization by servicing in orbit using trained engineering personnel."

As noted in this report (p. 59) one type of astronomical facility that is "clearly needed" is a long-wavelength radio telescope. In its thinking, the PSAC was apparently in concurrence with the findings of the Space Science Board of the National Academy of Sciences which met at Woods Hole, Massachusetts in 1965 and recommended that:

(1) "The National Academy of Sciences appoint a panel now to study possible conceptions" of a space radio telescope with an aperture of the order of 20 km, and

(2) "since the study recommended is for an ultimate space radio telescope, work should be started now that will lead to the use in space, within about ten years, of a high-resolution broad-band antenna system for radio-astronomical observations over the frequency range 10 MHz to a few hundred KHz."

In consonance with this second recommendation, work has been proceeding since 1965 on the conceptual study and technology development for a large-aperture paraboloidal-reflector low-frequency telescope (called LOFT). This work has delved into a number of areas in detail and led to the baseline concept shown in Figure 1. This report summarizes that work and describes the baseline concept.

THE LOFT RADIO ASTRONOMY FACILITY

Mode of Operation

The essential features of the projected operational LOFT facility are shown in Figure 2. Its central component is a large-aperture parabolic reflector surface which is deployed and contour-stabilized by a slow spinning motion around its axis of symmetry and which is orbiting at 6000-km altitude. Located near the focal point of the reflector is a broad-band "feed" system with matching receiver for primary data acquisition. Data is either stored or directly transmitted in real time to line-of-sight ground stations by a modulated high-frequency carrier for further data processing and interpretation.

An alternate mode of operation is shown in Figure 3. Here the orbiting reflector is employed as one receiver of an interferometer, working at frequencies above 10 mc. The other receiver is provided by any one of several existing ground-based radio telescopes. Information is coded with accurate timing signals and subject to post-acquisition analysis, or it is transmitted in real time for conventional interferometry. The relative motion of the orbital receiver with respect to the ground station provides additional information that allows suppression of undesired sidelobe signals from steady-state sources.

Alternatively, a second orbiting receiver can be used, as shown in Figure 4, to perform similar interferometric observations in the frequency band below 10 mc. Using two receivers orbiting in opposition and at 6000 km altitude each, this mode of operation can provide interferometer baselines as large as 24 000 km.

If fixed interferometer baselines are desired, one or more auxiliary receivers can be attached to the basic LOFT radio telescope by tie lines. A concept with four counterrotating interferometer stations is shown in Figure 5.

Properties of the terrestrial ionosphere can be investigated by turning the radio telescope toward the earth or toward the earth's horizon.

Finally, lunar occultation experiments can be conducted for the precise spatial definition of very small sources located

within a band of approximately ±2.5° from the lunar orbital plane, assuming the radio telescope is in an orbit of 6000 km altitude, inclined 45° with respect to the earth's axis (Fig. 6).

Scan and Track Capability

The orbiting structure is equipped with command receivers, attitude sensors, data-link transponders, power supply, and with an active pointing control employing electrical loop currents which provide orientation and spin torques by interaction with the geomagnetic field, as described in Reference 1, pp. 203-208. The wobble of the geomagnetic field (i.e., the deviation between magnetic and geographic poles) allows this system to cover the complete celestial sphere, including the polar regions. At the selected orbital altitude of 6000 km, scanning rates of approximately 180°/day are possible. This allows a complete radio mapping of the celestial sphere at 3° intervals within approximately 60 days. Optionally, object-fixed tracking can be provided for occultation experiments, for measurement of ionospheric diffraction and attenuation, and for continuous observation of discrete radio sources over extended periods of time.

A backup to this active orientation-control system is provided by the intrinsic orbital properties of the spinning reflector, as suggested by Fleig (Ref. 2). Because of the difference between roll and pitch inertia of the reflector structure, gravity gradient torques will cause a slow precessional scan of the pointing axis. If, in addition, the radio telescope is placed into an inclined orbit, the tesseral harmonics of the earth's gravitational field will cause precession of the orbital plane. The two effects combined can be shown to produce a continuous scanning motion of a celestial hemisphere. Calculations show that for a 6000 km orbital altitude, and a 45° orbital plane inclination, complete coverage can be obtained in approximately 500 days. Faster scans are possible if lower and/or eccentric orbits are used. Hence, if the active, geomagnetic control should cease to operate, passive scanning will continue and utility of the radio telescope for survey missions will be retained.

Orbital Altitude

An orbital altitude of 6000 km has been selected for the baseline as a compromise between several considerations.

In order to operate properly, the radio telescope must be sufficiently removed from the ionosphere, i.e., the local plasma cutoff frequency must be substantially below the frequency band of interest. Figure 7, taken from Reference 3, shows that the local plasma cutoff is below 0.5 mc at altitudes above one earth radius or above approximately 6000 km. A relatively high orbit is also desirable to provide large base lengths for operation of the radio telescope in the interferometry mode, and to widen the band of lunar-occultation opportunities. Conversely, it is necessary that a sufficient geomagnetic field exist for the active pointing and scanning control, and that both the gravity gradient and the tesseral harmonics of the gravitational field be sufficient to provide acceptable passive scanning rates. All of these effects diminish rapidly with increasing orbital altitude but are well within acceptable limits at 6000 km. Finally, the booster size required to inject the radio telescope increases with orbital altitude. For the present payload design weight, a Titan III launch vehicle is adequate to provide a 6000 km circular orbit.

Configuration and Size

The aperture (or dish diameter) of the radio telescope is determined by a desired half-power beam width of 3° at an operating frequency of 4 mc for which the Rayleigh relation yields a diameter of 1500 meters. This is considered adequate for a general mapping of the radio sky and for detailed observation of strong sources. For discrimination of fine structures and for extremely precise measurement of faint sources, interferometric operational modes will be used.

A full dish parabolic reflector, with a focal-length-to-aperture ratio of 0.5, has been selected in preference to other configurations of the basic radio telescope. This device has the advantage of broad frequency bandwidth, good sidelobe and backlobe suppression, retention of phase and polarization data, and utmost electronic simplicity. These factors are considered essential in providing a facility of long unattended life span in orbit, capable of many types of scientific observations which will be defined as the facility becomes operable.

With this choice, the burden of technology development becomes primarily one of structural design. Practical and credible methods must be devised to fabricate, package, deploy in space, and maintain adequate dimensional tolerances in a structure of

4

truly unprecedented size and performance.

The remainder of this summary status report will, therefore, be addressed to the problems of and solutions for very large, light-weight, efficient RF reflectors and to the technology associated with the development and operation of very large space structures for orbiting radio telescopes.

THE RADIO-FREQUENCY REFLECTOR

Weight Considerations

The magnitude of the task in constructing a reflecting surface of the required area can be visualized as follows: A parabolic surface having a diameter of 1500 meters and a f/D ratio of 0.5 covers an area of 1 873 000 square meters. Such a surface made from very thin, 0.001 in. thick, aluminum foil would weigh 138 000 kg, not including the required support structure.

From this it becomes obvious that a much more weight-effective means than that of a solid metallic sheet must be employed to remain within the payload weight limitations of present or foreseeable space boosters.

Fortunately, it is possible to obtain nearly perfect reflection of electromagnetic radiation from a gridwork of conductors, provided that the spacing between conductors is a reasonably small fraction of the wavelength and that the electrical surface conductivity is sufficiently good to prevent excessive ohmic losses in the induced reflector currents. A detailed analysis of the electromagnetic phenomena attending reflection on gridworks of widely spaced conductors has been performed by Robbins (Ref. 4). Results of this analysis have been substantially confirmed by experiments performed on parabolic-reflector scale models made from electrically scaled conductor grids (Ref. 5). The predictions of the analysis for the RF characteristics of large network reflectors are summarized briefly in the following paragraphs.

Resistive Losses

The finite conductivity causes a portion of the electromagnetic wave energy to be dissipated due to ohmic resistance and eventually to be thermally re-radiated in the infrared frequency range. As a consequence, the reflected RF wave will be attenuated in amplitude. As is shown later, if a material such as aluminum is used in the conducting elements of the surface, the ohmic loss can be kept at a very low level with acceptable total weights.

Inductive Losses

Intrinsic to a network of conductors is its electrical inductance which depends on the detailed geometrical properties of the conductors and of the network texture. Even for infinitely conductive grids, a portion of the impinging energy leaks through; the reflected energy is correspondingly reduced. Analysis shows that losses from this source can be kept low with reasonable conductor geometry and gridwork texture, provided that the spacing of individual conductors is 1/60 or less of the wavelength of interest. Even in the worst case, at the upper end of the frequency scale, i.e., at 10 mc or 30 meters wavelength, conductor cross-section dimensions of the order of only 2.5 mm are required, with the conductors spaced as much as 0.5 meter on centers.

One important effect of the inductance in a grid reflector is a phase shift in the reflected wave. Fortunately, for reasonably conductive reflectors, this phase shift is small and, in first-order approximation, inversely proportional to wavelength. The result is an apparent axial displacement of the reflector surface and a corresponding fixed displacement of its focal point.

Leakage

Transmission of RF energy through the reflector grid is of concern because the earth's ionosphere, and at higher frequencies, terrestrial thunderstorms and man-made RF signals will constitute a strong source of noise. With the radio telescope pointed away from the earth, the reflector must shield the receiver from becoming confused by such noise - in other words, the backlobe response of the radio telescope must be suppressed to the lowest practical level.

The same requirement must be satisfied if faint sources are to be observed, since the galactic background noise is by itself quite strong, and backside radiation transmitted through the reflector will be amplified by the intrinsic gain of the feed. Some directive backlobe response is associated with refraction around the rim of the reflector and is therefore unavoidable. It is desired that the additional noise from leakage through the reflector of backside energy not exceed this unavoidable source of data confusion. Analysis shows that this requirement is satisfied if the transmission through the net is kept below 2 percent of the impinging energy.

Figure 8 shows the result of a typical analysis. Ohmic and inductive power loss (or transmissivity) is plotted against the weight of a 1500-meter-diameter parabolic dish reflector grid made from thin aluminum ribbon conductors. The graph shows that satisfactory performance can be obtained with network reflectors which weigh only a small fraction of a solid-sheet reflector and that this component weight is well within the payload capability of existing space boosters. A weight of 300 kg will yield ohmic losses of less than 1 percent and transmissivity of about 2 percent at 4 MHz.

Choice of Conductor Network

Commercially pure aluminum is a preferred choice for the conductor material because it exhibits by far the highest figure of merit in terms of conductivity-to-weight ratio. Initially, attention was directed toward networks made from thin aluminum ribbons. Experimental work showed, however, that considerable difficulties would be encountered in producing and handling the extremely thin material, particularly in reliably producing many millions of joints while retaining reasonable structural integrity. Several alternatives were considered involving cable construction from ultra-fine wires and metal-polymer film composites such as those used in the ECHO I and ECHO II Space Flight Projects.

It was further recognized that the conductor material weight could be substantially reduced without significant loss in over-all performance by using aluminum in the form of ribbon conductors of sub-micron thickness. This clearly indicated the use of vacuum deposited films on thin plastic film substrates.

Aluminum deposits of micron and sub-micron range thicknesses were produced experimentally on thin (0.5 mil) polyimide (KAPTON*) films and found to have satisfactory properties. Networks can be produced from such films by a pattern of offset slits and subsequent transverse expansion by automatic processes well-developed in the expanded sheet metal mesh and plastic mesh industry. This avoids the cumbersome process of making joints; the network is an integral structure, bonded only at its edges to a supporting structure. Because it is originally manufactured from a flat sheet, it also has excellent "lay down" required for the folding and packaging process. Figure 9 shows a model of a conductor grid section in folded and expanded condition.

*DuPont Trademark

An analysis was made of the reflector weight, assuming a net made from various thicknesses and widths of polymer film ribbons coated with aluminum. The ribbon spacing and aluminum coating thickness was varied to yield a reflector transmissivity of 2 percent at 10 MHz. The results are shown in Figure 10. If this aluminum thickness is vacuum-deposited on both sides (for conservatism) of a 6μ (approximately 1/4 mil) thick film strip of 2.54 mm (0.1 inch) width, the mass-per-unit area varies as shown in the figure. The construction yielding minimum weight has an aluminum single thickness of 0.336μ and a ribbon spacing of 0.42 m. The associated total mass of polymer film and metal coating is 0.122 gram/m^2 or 227 kg for the complete reflector surface. Further decreases in reflector mass could be obtained by using a thinner polymer film substrate or by using still narrower and more closely spaced ribbons. The foregoing design, however, exhibits a power-reflectivity loss of 8 percent due to ohmic losses. (This is in contrast to a loss of 1.4 percent if the 227 kg of mass were entirely aluminum.) While this loss is acceptable, further reductions in the mass of aluminum would increase it and may, therefore, be undesirable. The design point shown on the figure was selected for subsequent concept definition.

Antenna Gain Patterns

An ideal parabolic reflector will form an interference pattern of reflected waves in the space surrounding the focal point. The characteristics of this interference pattern can be calculated by evaluating the appropriate Fresnel integral formula. The gain pattern of the antenna telescope is obtained by multiplication of the integrand with the illumination pattern of the feed system.

A real reflector will differ in its gain pattern from this ideal performance, primarily due to three reasons:

(1)   The feed system needs to be at least one-half wavelength in size. This blocks a portion of the incoming energy in the center of the aperture, resulting in some narrowing of the main beam, but also significantly increasing sidelobe response.

(2)   Because of its finite size, a broad-band feed system can not be placed exactly into the focus for all frequencies. Hence, for off-design frequencies, the response is defocussed and subject to chromatic aberration (i.e., the gain pattern becomes frequency

dependent in its detailed structure).

(3)   If the reflector deviates from a perfect parabolic
      surface, focus errors and phase errors occur between
      different portions of the reflected wave. Such errors
      again cause defocussing, "squint", astigmatism, and
      chromatic aberration of the radio telescope.

Geometrical imperfections can arise from manufacturing toler-
ances. These can be corrected or kept within tolerable levels by
appropriate design and quality control. Maximum deviations of 2
meters are tolerable and can be achieved by 1:1000 type of dimen-
sional control. Clearly, care must be taken to "know" to a high
degree of accuracy what the lengths of the important members in
the reflector will be after they are fabricated, packaged, de-
ployed, and subjected to long-time space exposure.

Deformation also occurs due to dynamic response of the struc-
ture to applied forces. Major sources of such forces are:

- Differential thermal expansion

- Gravity gradients

- Photon pressure

- Steady state and transient control torques.

Analysis shows that the dynamic response to space-fixed excitation
forces takes the form of backward traveling waves in the rotating
system. A detailed study of the resulting network deformation for
a typical configuration has been performed (Ref. 1 and 5). Re-
sults show that amplitudes of excited deformation modes stay well
below a 2-meter value for most cases, and therefore are not likely
to generate appreciable gain pattern distortions.

A systematic deviation from parabolic shape occurs in the
present design because, for structural reasons, the inner portion
of the reflector cannot be a perfect paraboloid; approximations
consisting of a series of cones (or near cones) must be employed.
One such configuration is discussed in detail in the next section.
Its surface deviates from the true paraboloid by less than 2
meters over most of the reflector and has a maximum error of 11
meters over a small portion near the center.

The influence of such deviations on the gain pattern is an obvious design criterion. Estimates can be made by evaluating the complex Fresnel integral, accounting for the phase shifts due to geometrical deviations of reflector and feed systems.

Gain patterns have been calculated for the reflector shape described in the next section, assuming a parabolically tapered aperture illumination, declining from a maximum at the center to zero at the rim. Aperture blocking due to the feed was assumed to be circular, with a blocking diameter equal to 60 percent of the wavelength. It was further assumed that the feed system would be located such that the 10 MHz portion would be exactly in the focal plane, and that the 4 MHz and 1 MHz portions would be behind the focal plane by 35 percent of the corresponding wavelength. These assumptions are consistent with the trapezoidal-tooth, log-periodic feed concept discussed in Reference 1. Data shown in Figure 11 are plotted for easy comparison on a non-dimensional azimuth angle scale. The gain pattern of an ideal parabolic reflector without feed blocking or displacement is also shown.

The results of these calculations show that a first sidelobe suppression below 20 db over most of the frequency band of interest is practically feasible. This compares to 24.7 db for an ideal reflector surface without blocking effect.

Improvements can be gained by better tailoring of the aperture illumination. Such tailoring can be effected, for instance, by reducing the RF reflectivity of the reflector near the rim at the possible expense of increased backlobe levels due to transmissivity.

The effect of a quartic $((1-r^2)^2)$ aperture illumination is shown in Figure 12. It appears that for this type of illumination sidelobe level, suppression of -25 db can be reached in the center of the frequency band of interest at the cost of some mainlobe broadening.

Some additional improvement potential, particularly at the upper end of the frequency band, appears possible in this case by further optimization of the cone-paraboloid approximation. For instance, additional back stays can be employed further to improve the shape, particularly if better RF performance in the higher frequency range is desired. Alternatively, a relatively small, separate, flat disk reflector could be used to reduce the

11

11.0 meter apex deviation of the single back-stay configuration. Such improvements will be weighted in future studies against penalties attending the additional structural complexities and may be traded off with similar improvements possible by more sophisticated feed design and electronic means of contour correction.

The accuracy of the theoretical approach used in obtaining the foregoing results has been substantially verified by RF pattern tests with scale models. These models consisted of solid reflectors in configurations of complete parabolas, parabolas with central openings, and parabola-cone combinations illuminated by simple dipoles and by trapezoidal-tooth log-periodic feed systems (Ref. 5).

STRUCTURAL DESIGN AND TECHNOLOGY DEVELOPMENT

The Baseline Configuration

The structural baseline configuration is subject to change as the design evolves and as results from analysis and test programs become available. Another source of change is a continuing dialogue with the prospective user, that frequently refocusses attention to specific performance requirements which become more quantitative as the design matures. This is typical for a long-range development program; therefore, any "baseline" configuration is at best a compilation of selected concepts which, at the moment, appear best suited to achieving the desired characteristics and are mutually compatible in the sense of systems integration. The baseline configuration discussed here is no exception and must be considered not as a fixed, final design, but as a feasible and credible version thereof, suitable for a detailed engineering analysis and test evaluation program.

An overall view of the structural-design configuration and its principal dimensions are shown in Figure 13. A summary of design characteristics and component weights is given in tabular form.

Baseline LOFT Concept

DIMENSIONS:

Deployed	1500 Meters Diameter, 1020 Meters Length
Packaged	5.5 Meters Diameter, 5.9 Meters Length

GEOMETRY AND MATERIALS:

Reflector Net
> Paraboloidal Outside 50% Radius; Tangent Cone from 50% to 40% Radius; Secant Cone to Center. Maximum Deviations from True Paraboloid: -2 Meters at 40% Radius, 2 Meters at 25% Radius, -11 Meters at Center.

> Stainless Steel Support Net and Back Stays: Trifilar tapes, each 0.02 in. by 0.5 mil. 240 Meridionals, 40 Circumferentials, 240 Back Stays (see Fig. 14).

> Conductor Grid: 0.275 Micron Aluminum, Vacuum Deposited on Both Sides of 1/4-mil Polyimide Film Slit to 0.1 in. Width. 40 cm Deployed Spacing. (See Fig. 9)

Rim Mass
     Stranded Aluminum Cable, Multi-Turns

Front Stays
     120, 0.75 in. by 0.5 mil Polyimide Tapes

Central Mast
     3.04 meters Diameter, 760 Meters Length
     Aluminum Tubing Braced with Aluminum Tape Diagonals

LAUNCH MASS

Support Net	43 kg
Conductor Grid	239
Back Stays	12
Rim Mass	227
Front Stays	37
Main Mast	250
Back Mast	25
Feed System	200
Front-Stay Bobbins	50
Support Structure, Mast Canisters	300
Octoroid System	100
Back-Stay Bobbins	50
Spin-Up Subsystem	300
Power Generation and Storage	300
Control System	150
Data Handling and Communication	50
Launch Shroud (Portion Chargeable to Payload)	320
	2640 kg

The Reflector Structure

Concept. - A detail of the reflector network in the vicinity
of the reflector rim is shown in Figure 14. It consists of a net
of flexible stainless steel cables supporting a "non-structural"
gridwork of aluminized ribbon conductors. The basic support
structure consists of 240 radial cables connected by 40 parallel
circle cables. Joints between the two sets of cables are pre-
cisely located to ensure metric accuracy of the surface.

The supporting cables are of tri-filar construction. Each
strand is made from a flat, thin ribbon and spaced from the others

14

as shown by the inset of Figure 14, tied by spotwelds at approximately 1-meter intervals. This provides a redundancy of the cable construction and, for practical purposes, eliminates the danger of serious contour degradation by accidental failure. Hinged joint rings provide the connections at points of intersection of the support grid.

The conductor grid fills in the panels made by the support net. It consists of the aforementioned aluminized polyimide slit panels (Fig. 9) which are mounted to allow slight billowing. As previously discussed, such a configuration is satisfactory for RF reflectivity.

The micrometeoroid fracture hazard of thin wires and flat tapes used in the reflector network construction has been analyzed by R. MacNeal (Ref. 6). The results of this analysis applied to reflector ribbons and to a tri-filar support cable system are shown in Figure 15.

A reasonable number of fractures can be tolerated for the reflector grid without noticeable degradation of radio-telescope performance. For instance, the analysis shows that a mesh made from conductors 2.5 mm wide and 6 microns thick will experience only about 450 fractures a year. In ten years, this averages only about one fracture per 20 m by 20 m panel. Thus, performance degradation from this source will be small. Fracture of supporting cable elements will be more serious since they are likely to cause contour deviations exceeding the postulated two-meter value. The design of the cable construction has been selected to produce a single-fracture probability of less than 1 percent in four years of life time in orbit. Fracture experiments with hypervelocity particles impacting on flat tapes and on composite tape-cable construction will be required in future work to verify the theoretical predictions.

Deformations and Packaging. - An essential feature of the reflector structure is the fact that it is centrifugally pre-stressed by rotational motion. The centrifugal-force field associated with this motion must be considered as a portion of the structure, contributing significantly to ability to resist deleterious deformations from environmental forces, much in the same sense as the inflation pressure which provides structural integrity to a pneumatic tire, to a blimp-type airship, or to any other pressure-stabilized, load-carrying structure.

A rotational speed of one revolution in 11.4 minutes has been selected, corresponding to a linear velocity at the rim of approximately 14 meters/sec. This speed was selected as a compromise -- fast enough to generate tensile stresses sufficient to keep the flexible network members adequately taut and to avoid dynamic coupling with the much slower orbital frequency, but sufficiently slow to keep the demand for orientation control torques at tolerable levels. The effect of centrifugal stiffening is clearly evidenced by referring to the planform of the reflector grid shown in Figure 13. The basically quadrangular network texture has no direct (i.e., elastic) constraints against deformations where parallel circles rotate relative to each other. For this reason, the original baseline configurations which have been described in previous reports (see Ref. 7, 8, and 9) used triangular mesh textures. A detailed analysis of the dynamic deformations produced by environmental forces showed, however, that the shearing stiffness provided by the diagonal elements were not significantly greater than the stiffening effect derived from centrifugal force. In fact, calculations showed that the deleterious out-of-plane motions of the surface were reduced by deleting the diagonal stiffening members, since, in this case, vibrational energy goes preferentially into the innocuous in-plane mode of deformation.

A second, and more significant advantage of the selected net texture is its capability to undergo large (90°) shearing deformations by joint rotation alone, without requiring in-plane strains or creases in the material. These characteristics allow a solution to the packaging problem without recourse to creasing or loose-loop formation in the net. The kinematic process of the packaging and deployment concept is shown schematically in Figure 16. It involves a relative speed differential in the reel up of adjacent radial cables, causing a complete 90° shearing collapse of the network into a narrow strip as each net section enters the "octoroid" package reel.

This reel-up method is also suggestive of a feasible fabrication concept. The network of support cables is fabricated from pre-marked cable lengths, beginning at the central portion of the reflector, and the conductor network, made from slit aluminized sheet, is attached to the panels. As each circumferential row of panels is complete, it is inspected and reeled on the octoroid assembly. By this method, the fabrication area need not exceed a circle of approximately 20-meter radius. The fabrication and packaging proceeds continuously and simultaneously, somewhat analogous to the process employed in printing a daily newspaper.

The centrifugal-force field provides stress components in planes normal to the paraboloid's axis. Axial stress components must be provided by the central mast structure and transferred to the reflector net by the front tensioning tapes and by the back-stay system.

Because the total axial component of the membrane stresses is constant, the meridional stress in a paraboloidal membrane must increase indefinitely as the apex of the paraboloid is approached. To satisfy local equilibrium, the circumferential stress must correspondingly decrease and eventually assume large negative values, i.e., the parallel circle members would have to carry compressive loads. This is clearly not possible for the flexible cable construction employed in the reflector. Analysis shows (Ref. 9) that circumferential stresses will change sign at approximately 50 percent of the rim radius, and from there on inward the only possible tension structure for a simple membrane without circumferential stress is that of a tangent cone. As shown by analysis and RF experiments (Ref. 5) this configuration does not yield acceptable gain-pattern performance.

The approximation to a paraboloid can be improved by judicious choice of the back-stay system which allows the tension membrane to assume the shape of a compound cone. A configuration with a single set of back stays is shown in Figure 13 and has been chosen for the current baseline concept.

The Central Mast Structure

One of the most challenging design tasks for the radio telescope is presented by the central mast structure. The mast provides the axial tensioning component for the network structure. It is therefore subject to compressive loads and consequently to instability failure modes. This is compounded by vibratory resonance (critical speed) due to the structure's rotation. In addition, the structure must be automatically erected from a package that is no more than approximately 3 meters in diameter. The ultimate design load, P, including a safety factor of 1.5 is 5.2 newtons (1.16 lbs) and the span, L, between loads is approximately 760 meters or 2700 ft. This results in a structural load index, P/L^2, of 1.3×10^{-10} psi.

This index is many orders of magnitude lower than would be found in conventional design practice, and there is very little recourse to applicable experience in deciding upon a suitable design configuration. However, it is clear from the outset that for reasonably dimensioned structural members, the working stress levels will be exceedingly low and that considerations of foldability, elastic stability, and initial imperfections will dominate the detail design. An open lattice column appeared to be desirable, since it minimizes thermal distortions from differential solar heating and since it concentrates the structural material into relatively compact individual elements. Such a column design is shown in Figure 17. It consists of three longerons connected by swivel joints to triangular batten frames at regular intervals. A detail of the swivel joint is shown in Figure 18. Shearing and torsional stiffness is provided by diagonal tension members in the rectangular panels formed by adjacent longerons and battens.

A detailed design analysis and structural test program for a lightly-loaded lattice mast has been reported in Reference 1. It was observed that deviations from geometrical perfection (i.e., initial bows) in individual members and in the overall mast alignment profoundly affect the structural performance in terms of rigidity and resistance to local or general elastic buckling. On the basis of these studies, straightness requirements were postulated. For individual members, the initial bow is not to exceed a value equal to the radius of inertia of the cross-section (i.e., 0.173 in. for 0.5 in. tubing). For the total mast assembly the initial bow is not to exceed four radii of inertia (i.e., 4.25 meters) or approximately 0.5 percent of the total mast length. This last condition will require careful rigging and optical checkout of the mast assembly.

A design tradeoff is provided in the selection of the distance between adjacent batten frames. Close spacing allows the longerons to be made lighter because of the increased frequency of supports provided by the batten joints; however, the number of batten frames and joints, and their associated weight is correspondingly increased. Figure 19 shows the mass variation of batten frames (including joints) and longerons versus batten spacing, assuming aluminum tubing with wall thickness of 0.01 in. as design elements. A minimum total mass is obtained for a batten spacing of approximately 2.5 meters. The design value of 2.6 meters has been selected to reduce the number of joints at a negligible penalty of overall weight.

Because of the very light structural loads imposed upon the mast, the individual components can be made from very slender, thin-walled aluminum tubing. This is exploited in the package and deployment mechanism as shown in Figure 20.

In the packaged configuration, the three longerons are elastically bent into a tightly compressed coil circumscribing the triangular batten frame with each frame rotated by an appropriate angle, with respect to its adjacent frame. This configuration can be shown to be metrically equivalent to the deployed condition. The mast structure can go from the packaged to the deployed condition by a transition in which the distances between batten frame joints are reduced from their nominal value of 2.64 m by approximately 8 percent. This is accomplished by radially inward-directed forces exerted upon the three batten frame joints by compression pulleys. These forces cause the three battens to buckle elastically in the transition section of the deployment mechanism and the diagonal members to become temporarily slack. As the mast emerges from the transition section, the battens will elastically recover and become straight in the deployed configuration.

The deployment canister is provided with a rotary drive which turns the packaged portion, thus feeding the mast longerons in a helical, space-fixed path into the transition section. Three straight belt assemblies engage a short section of the deployed mast, providing positive motion. This straight section also provides the cantilevered base support to the external deployed mast.

A photograph of the transition section of a scale model is shown in Figure 21. A complete mast and deployment assembly similar to that described here is shown in partially deployed condition in Figure 22.

Packaging and Deployment

A packaged configuration of the LOFT structure is shown in Figure 23. The overall package dimensions have been chosen to fit into a modified Titan III booster payload shroud. The package is arranged around the central mast-deployment canister. The reflector network is packaged on the octoroid assembly which, in turn, is supported from the base plate of the mast canister. Front stays and a portion of the back stays are packaged on their respective bobbin rings, the rim structure is placed along the

19

periphery of the central mast canister. A separate deployable mast assembly supports the back-stay bobbin ring and a similar deployable spin-up-motor support structure extends from the front end of the central mast.

After ejection of the booster shroud, the spin-up-motor support is extended and the spin-up propulsion system is ignited. As torque is transferred to the package, the reflector rim pulls away in a radially outward motion, controlled by payout of the front stays and reflector net.

After the reflector rim has cleared the package and adequate spin rate has been reached, the central mast and back-stay support are partially deployed to avoid interference between the various portions of the structure (Fig. 24).

Figure 25 shows, schematically, the further course of reflector-net deployment. Angular momentum is continually transferred from the spin propulsion system through the front stays to the reflector, and radial deployment is continued. During this phase, the backwound portion of the back-stay cables are transferred to the back-stay bobbins. The spin propulsion system is programmed to provide the total angular momentum to the LOFT structure at a time when approximately 60 percent of the reflector is deployed. The propulsion system is then shut down and the radial deployment continued. Coriolis forces now slow the rotational speed, as the network is deployed into an approximately flat disk. When the full radius is reached, the radial deployment ceases and the circumferential support cables become taut.

The central mast and back-stay support are now fully extended, bringing the reflector network to its desired geometrical contour by pulling the radial support cables taut. After the final phase of the mast deployment, the feed network structure is deployed from its package. The complete LOFT structure is now ready for in-flight checkout and operation. Calculations show that the complete deployment sequence can be accomplished in less than two days (Ref. 1). Improved controls allow a reduction of this time, if desired, to approximately two hours.

Ground- and Flight-Test Evolution

A major task ahead is associated with the enormous size (as scaled by the human body) of the radio telescope structure. This

causes psychological as well as technical problems, particularly since it must be frankly admitted that there is no practical method in sight that would allow the structure to be fully deployed and inspected in ground test facilities, let alone be subject to the full-scale, simulated systems tests which have become accepted practice in more or less conventional space systems hardware development. This situation is compounded by the use of rotational motion as a means of structural stabilization in free space. While the effects of a centrifugal-force field upon a structure and the structure's dynamic response to disturbing effects is no less subject to deterministic prediction than that of simple gravity loads on equally large civil engineering structures such as dams, suspension bridges, domes, etc., they are much less accessible to the intuitive appraisal by a majority of the technical community.

Finally, the proposition of a structure that consists of a diaphanous network made from millions of thin ribbons and wires invokes the idea of inexorable snags and snarls for which there exists very little in the way of rigorous engineering analysis procedures (Ref. 10).

From this it is clear that a carefully paced evolution of technology must take place in the form of tests and experiments with engineering models of increasing size and complexity.

A 2-meter-diameter reflector net and front stay assembly has been constructed and tested by spinning in a rotary chamber (See Fig. 26). Good contour accuracy and stable dynamic response characteristics are evidenced in these tests.

A 5-meter (1/300 of full scale) model has been designed (Fig. 27) and is presently under construction. The size was determined as the largest scale model that could be reasonably tested in a large vacuum chamber at sufficiently slow speeds to keep stresses in the desired range, but without incurring significant gravity effects. It contains all the essential structural components including deployment mechanisms for mast, octoroid assembly, and front-stay bobbins. This model will be deployed from a rotary table in a large vacuum chamber. Provisions are made to excite the spinning model by a variety of disturbing forces and to record the time sequence of network surface deformations associated with these disturbances. A detailed dynamic analysis of predicted responses is conducted, using the same theoretical methods

used in the structural dynamics analysis of the full size structure. Correlation between experiment and prediction is expected to validate the theoretical analysis.

CONCLUDING REMARKS

Clearly, proving the feasibility and exploring the technology required to build LOFT will necessitate flight tests. An obvious step in this direction is to fly the 5-meter model as a payload on a sounding rocket such as the Aerobee 150. Preliminary study indicates that deployment in a scaled realistic fashion, testing of structural dynamics, and recovery of film would be possible during the several available minutes of zero-g vacuum conditions.

Larger structural models (50 to 150 meters) will be required to prove out realistic materials, joints, fabrication, packaging, and deployment. Here, for the first time, the structure cannot be ground tested as a whole before launch. Such testing could be aided tremendously by being done as part of a manned orbital space program. Intelligent observation and interaction with the deployment process of the larger-scale reflector structures appears to be eminently desirable. Particularly, the Apollo Applications (AAP) manned flight program provides a system by which man's ability to observe, interpret, and act intelligently can validly be applied to the development of non-ground-testable space flight hardware (Ref. 10).

REFERENCES

1. Engineering Staff: Study of an Orbiting Low Frequency Radio Telescope. Astro Research Corporation Report ARC-R-262, November 22, 1967.

2. Fleig, A.: Private Communication.

3. Carpenter, D. L.: Proceedings of 14th URSI General Assembly, 1963.

4. Robbins, William M., Jr.: Gratings and Networks of Ribbons as Radio Reflectors. NASA CR-872, September, 1967.

5. Engineering Staff: Design, Analysis and Testing of Models of an Orbiting Low Frequency Radio Telescope. Astro Research Corporation Report ARC-R-268, December 15, 1967.

6. MacNeal, Richard H.: Meteoroid Damage to Filamentary Structures. NASA CR-869, September, 1967.

7. Schuerch, H.: Large-Sized Orbiting Radio Telescopes. Proceedings of XVII Congress of the International Astronautical Federation, 9-15 October 1966, pp. 165-176.

8. Robbins, William M., Jr.: The Feasibility of an Orbiting 1500-Meter Radio Telescope. NASA CR-792, June 1967.

9. Robbins, William M., Jr.: Spinning Paraboloidal Tension Networks. NASA CR-873, September, 1967.

10. Schuerch, H.: Some Considerations of Manned Extra-vehicular Activities in Assembly and Operation of Large Space Structures, NASA CR-871, September, 1967.
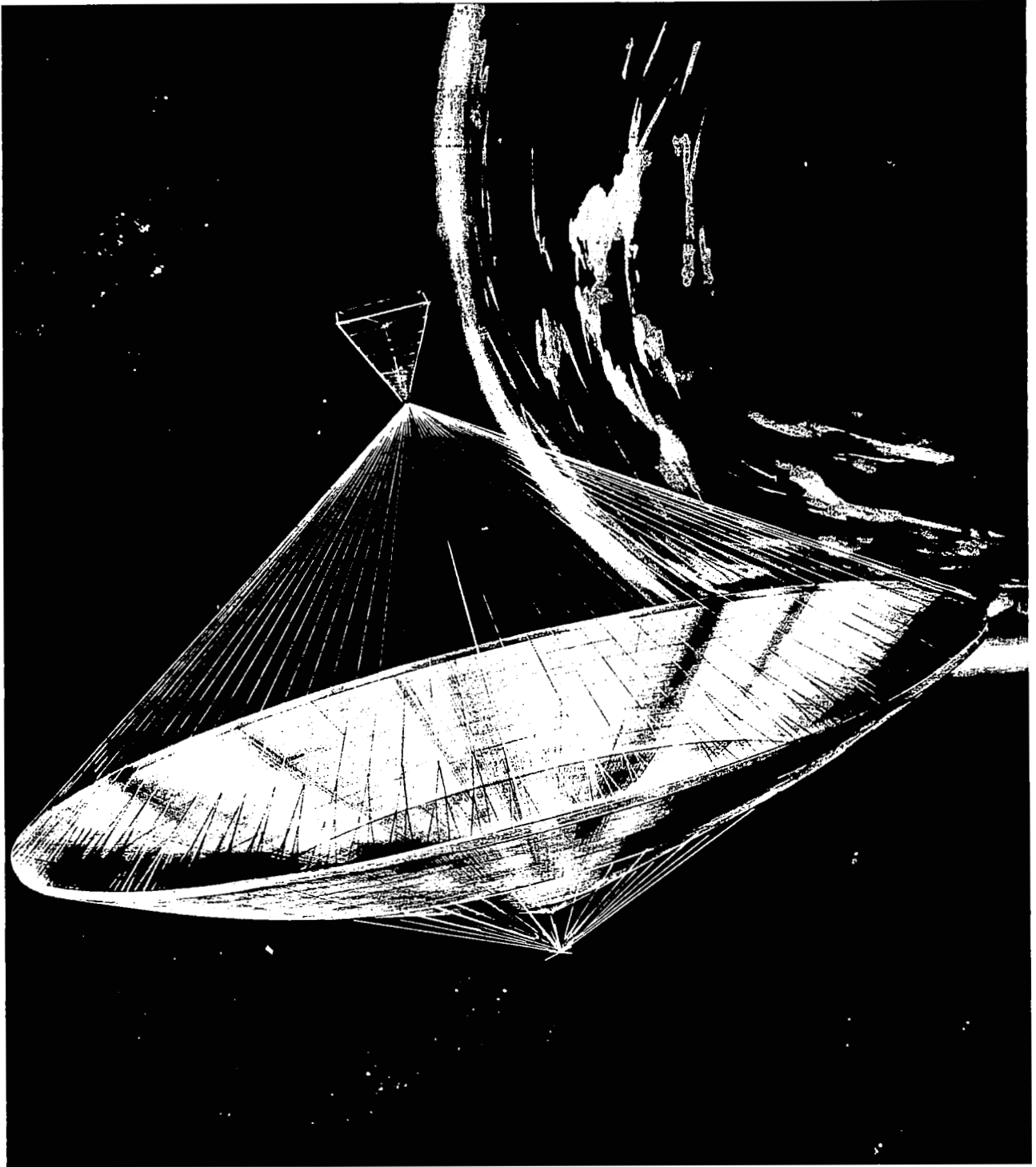
Figure 1.   LOFT Baseline Concept

25
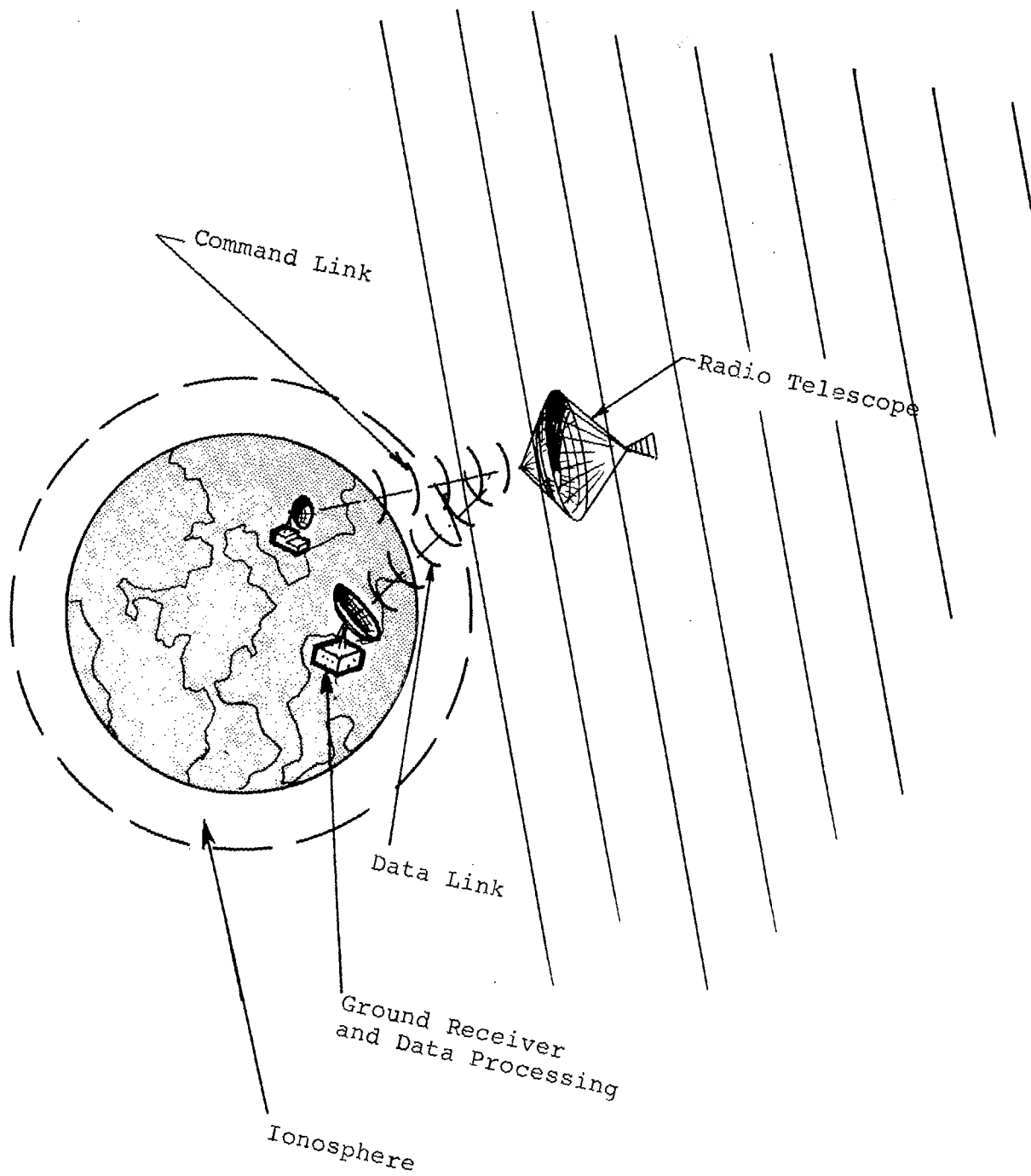
Figure 2. Orbiting Radio Astronomy Facility
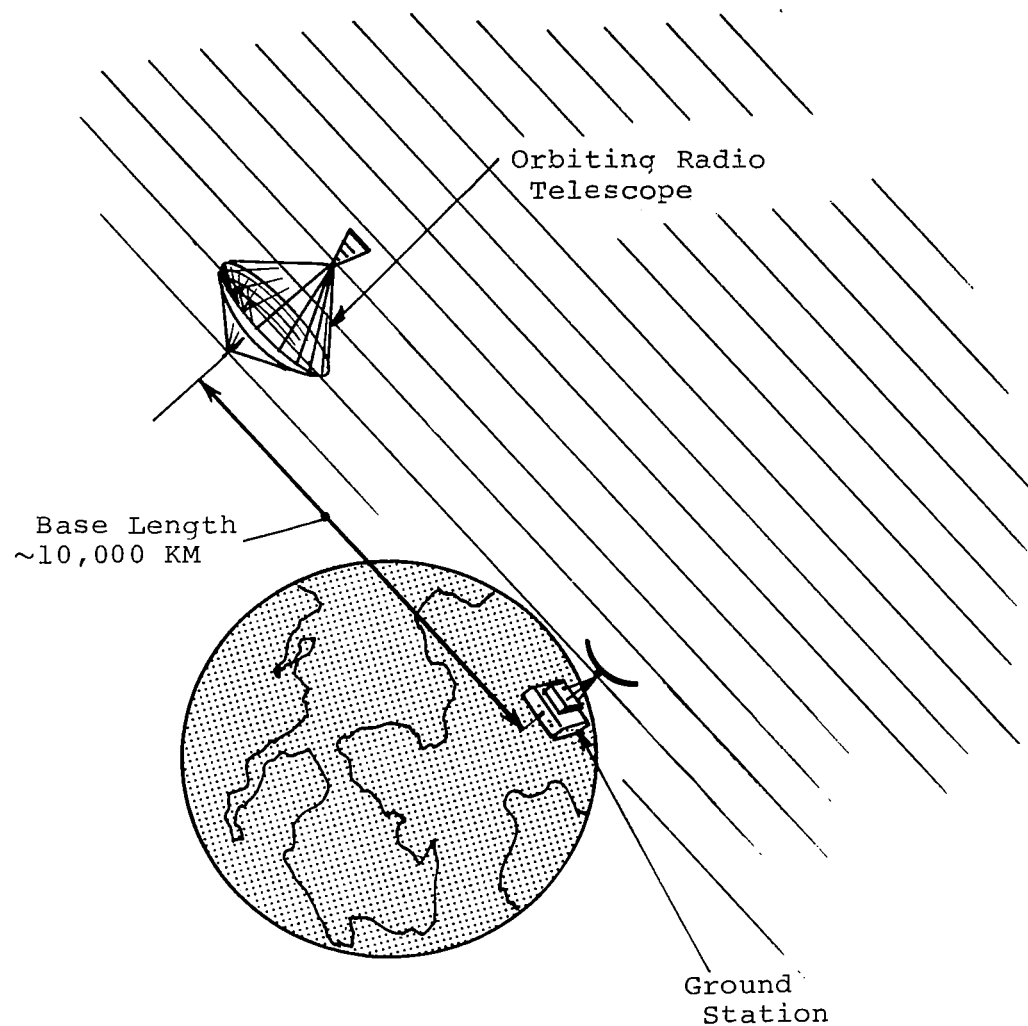
Figure 3.   Operation in Interferometry Mode With
             Ground Station at Frequency > 10 MHz

Base Length –
24 000 km
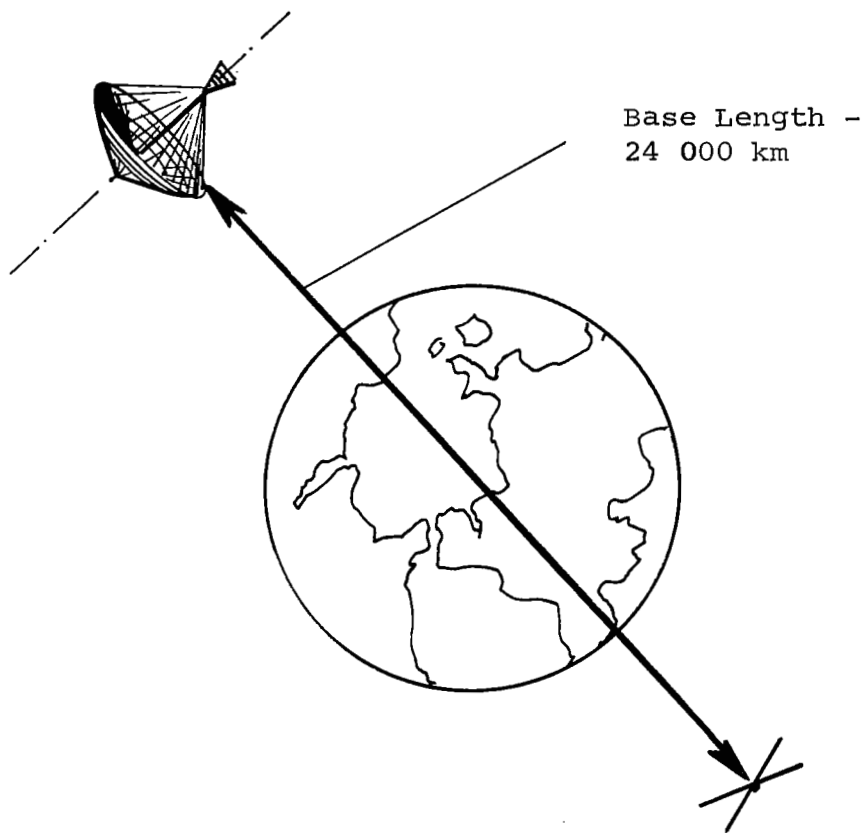
Figure 4.   Operation in Interferometry Mode With Second
Orbital Receiver at Frequency < 10 MHz
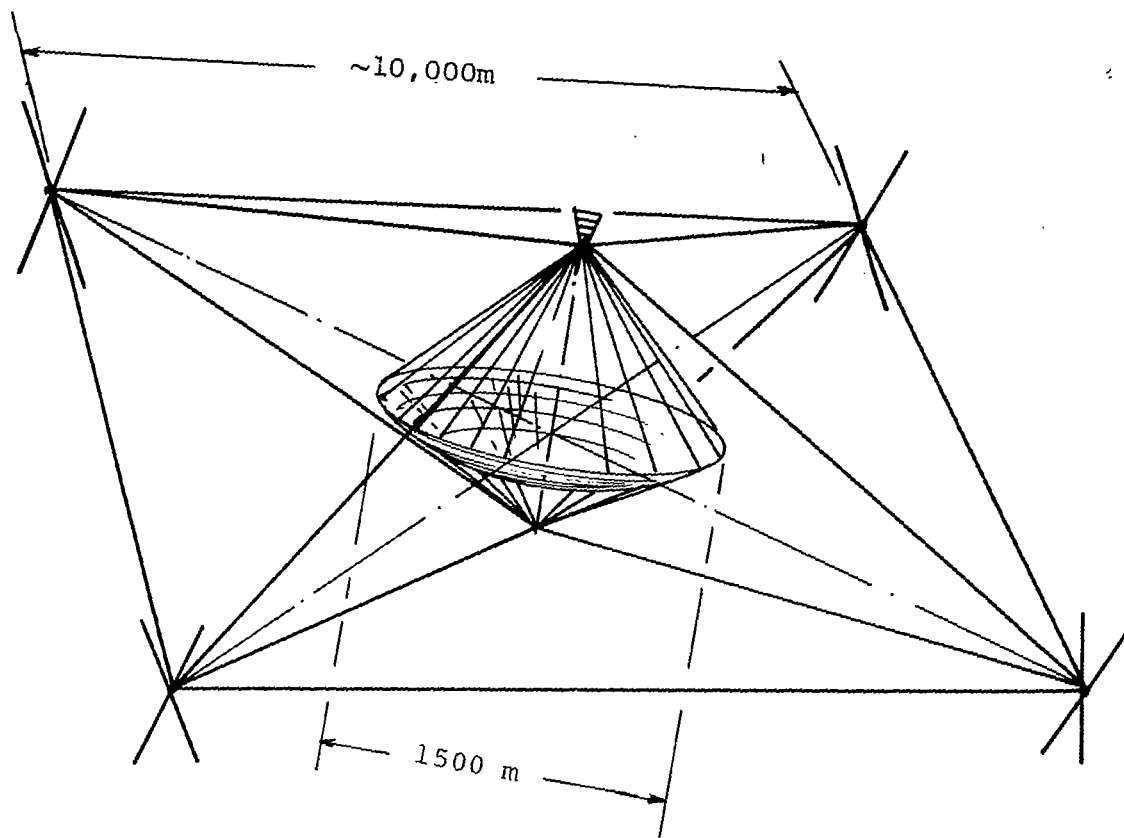
Figure 5. Loft Concept with 4 Counter-Rotating Outrigger Interferometry Stations

Plane of Lunar Orbit

Plane of Loft Orbit

23.5°

Ecliptic

45°

N

S

6000 km

Moon

Maximum Band Width of
Occultation Opportunities
~ 5°

384,400 km
(not to scale)
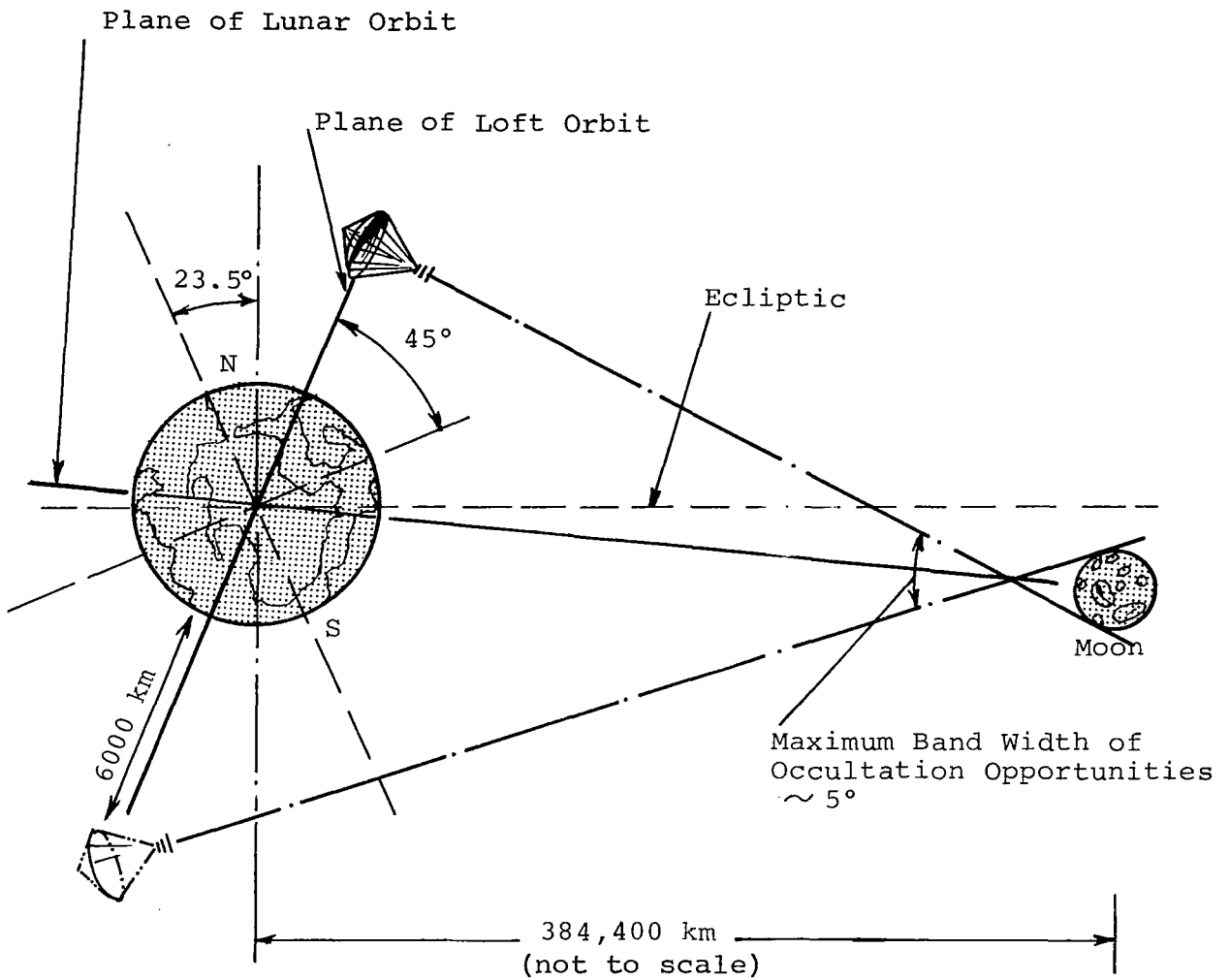
Figure 6.   Lunar Occultation Experiment from
Orbital Receiver
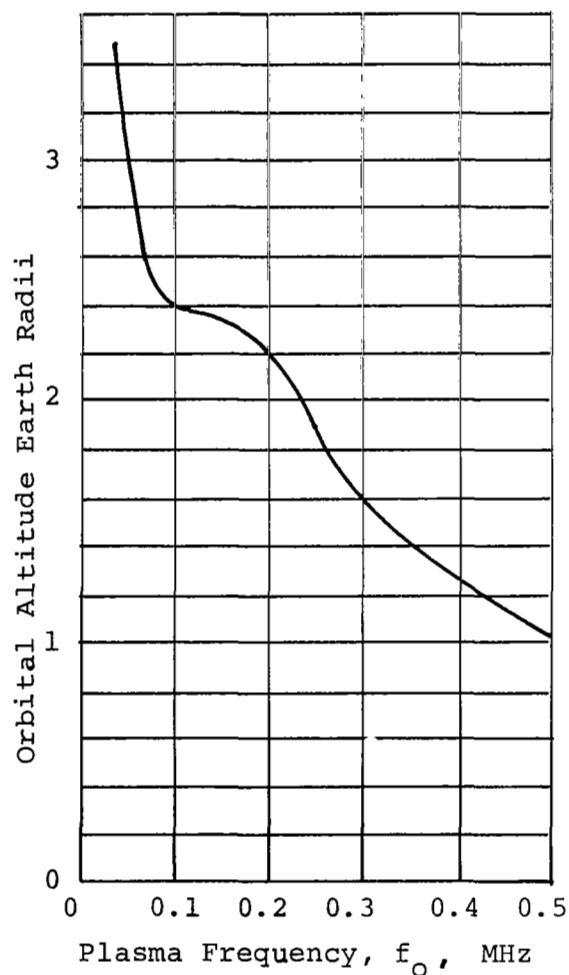
Figure 7. Plasma Frequency as a Function of Altitude. Derived from the Equatorial Profile of Magnetospheric Electron Density
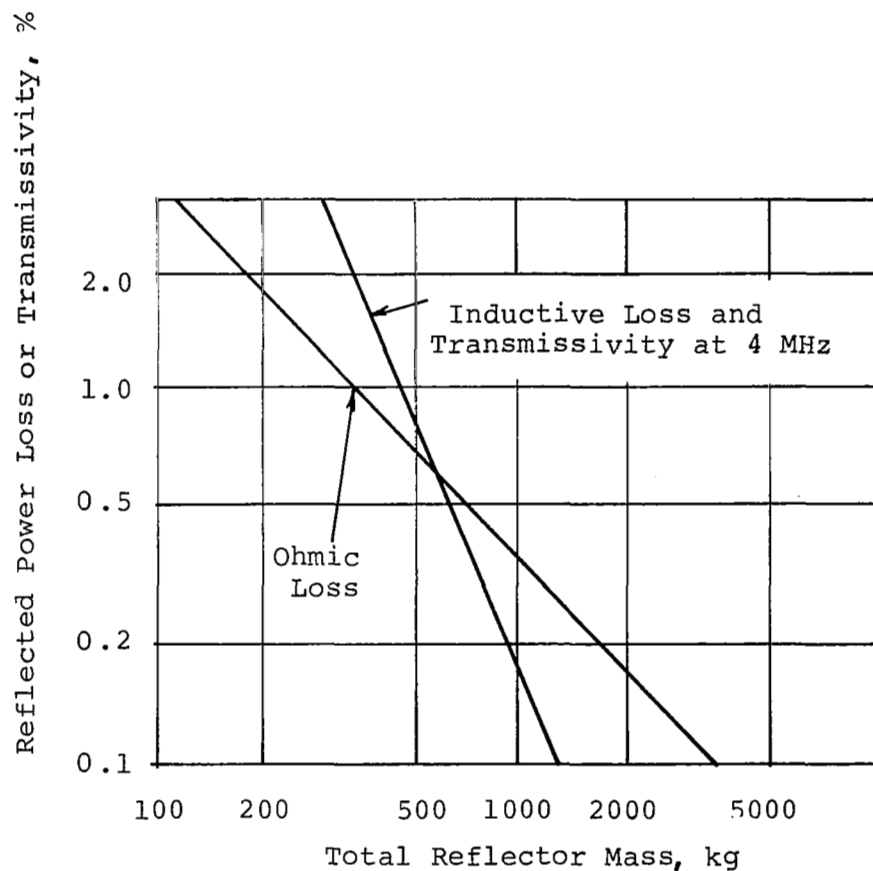
Figure 8. Geometrical and Ohmic Power Loss vs Conductor Mass for 1500-Meter Reflector Made From Aluminum Ribbon Gridwork. Ribbon Dimensions: 0.1 x 0.0005 in.
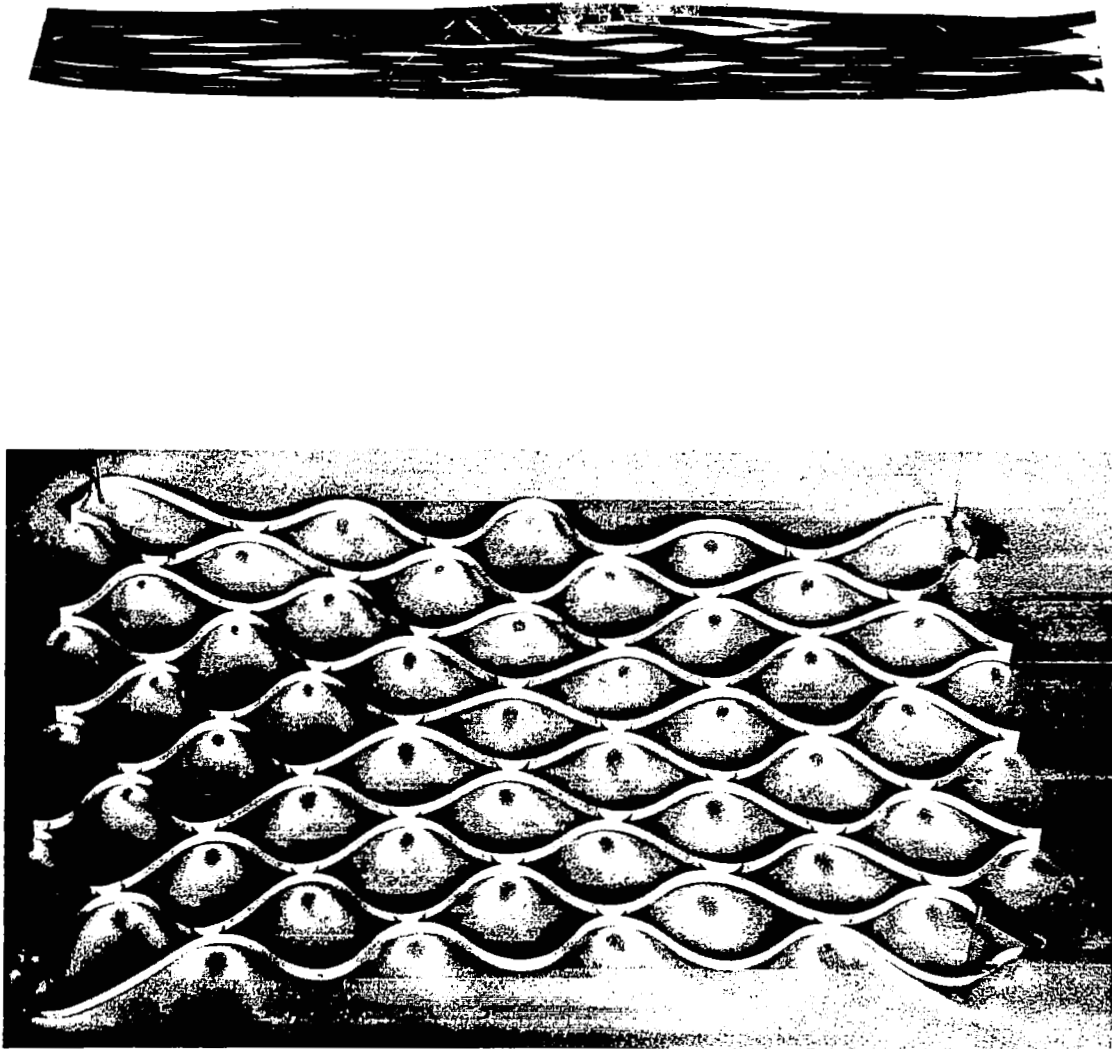
Figure 9.   Slit Aluminized Polymer Film Conductor Grid
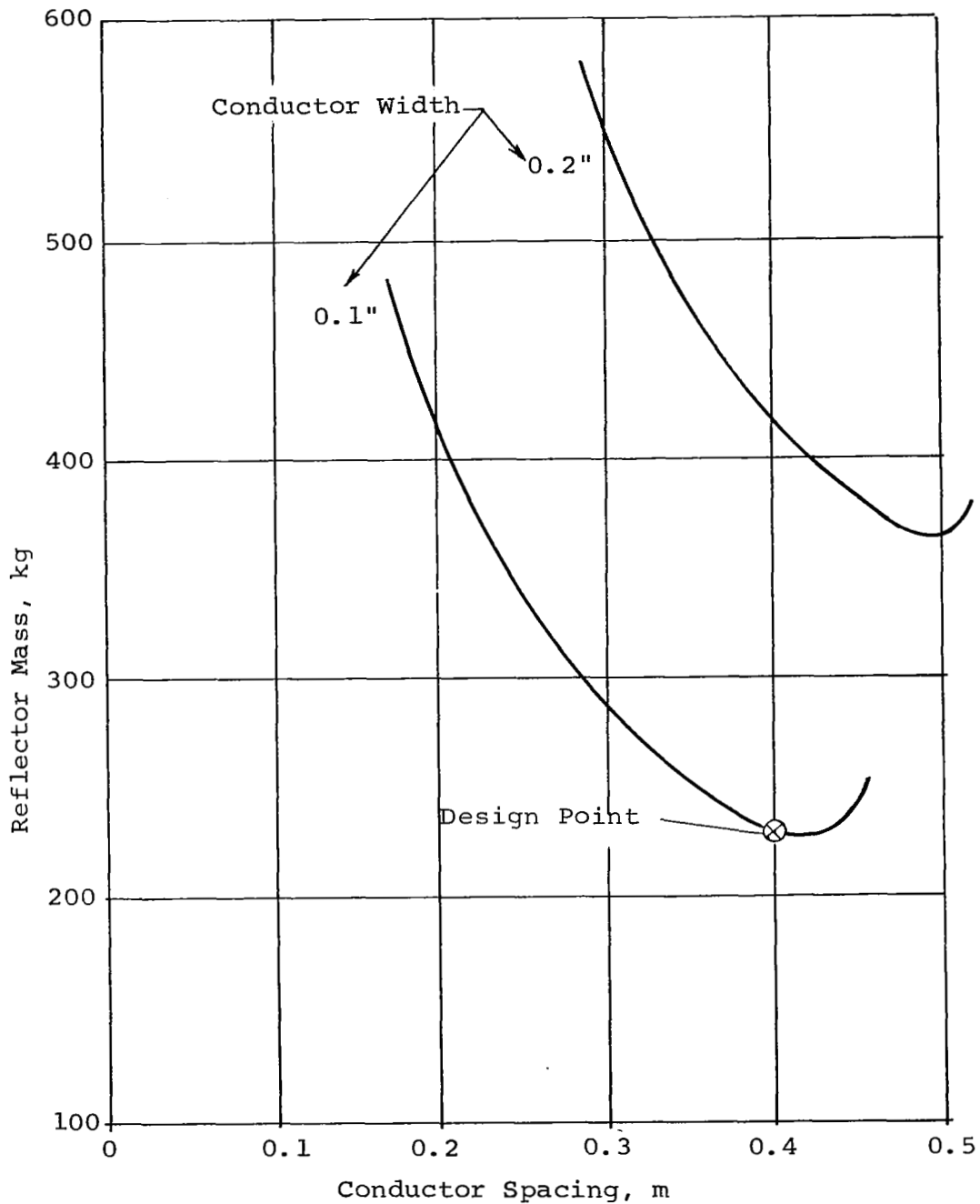
Figure 10. Mass of Conductor Grid vs Conductor
Spacing for 1/4 Mil Polymer Film
Coated with Aluminum. Transmis-
sivity: 0.02 at 10 MHz.
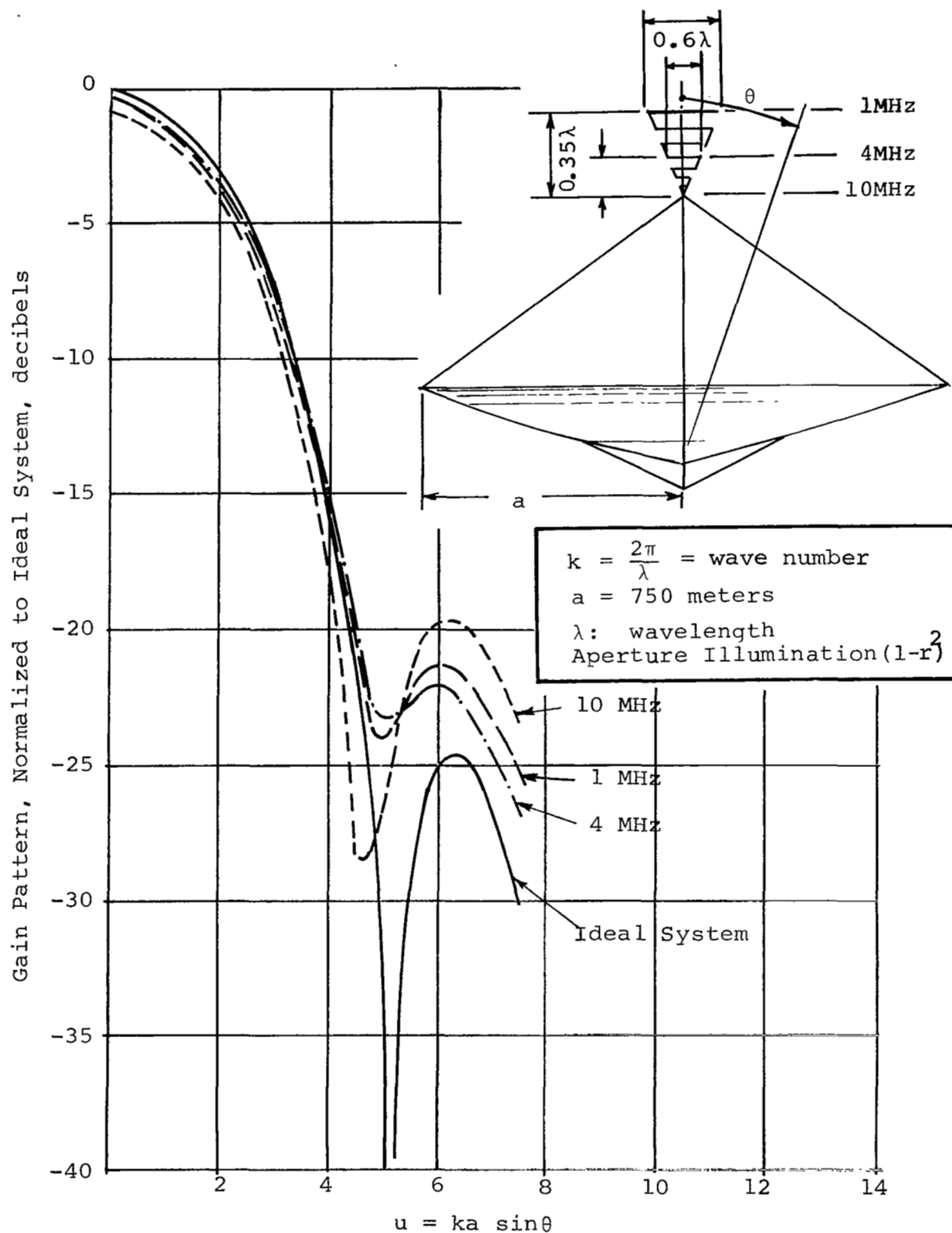
Figure 11. Effect of Reflector Shape and Feed System, Parabolic Illumination Taper
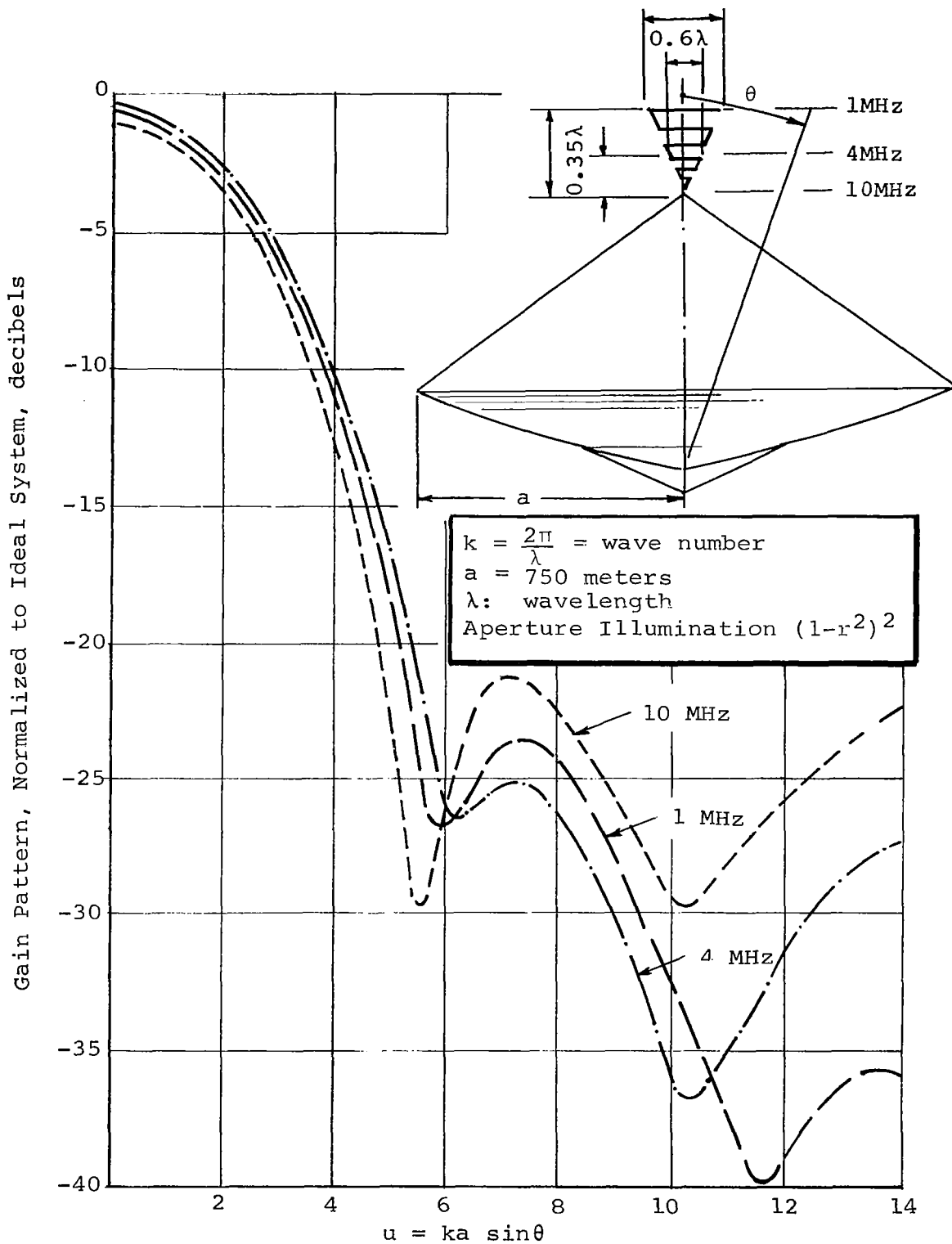
Figure 12. Effect of Reflector Shape and Feed System, Quartic Illumination Taper

RIM MASS

REFLECTOR

COMPRESSION
MAST

.5 R

.4R

BACK
STAYS
21°

200 M

SUPPORT
NET
240 MERIDIONALS
40 CIRCUMFERENTIALS

CONDUCTOR
GRID

1500M

PYRAMIDAL
LOG-PERIODIC
FEED

FRONT STAYS

750 M

187.5 M

1020M
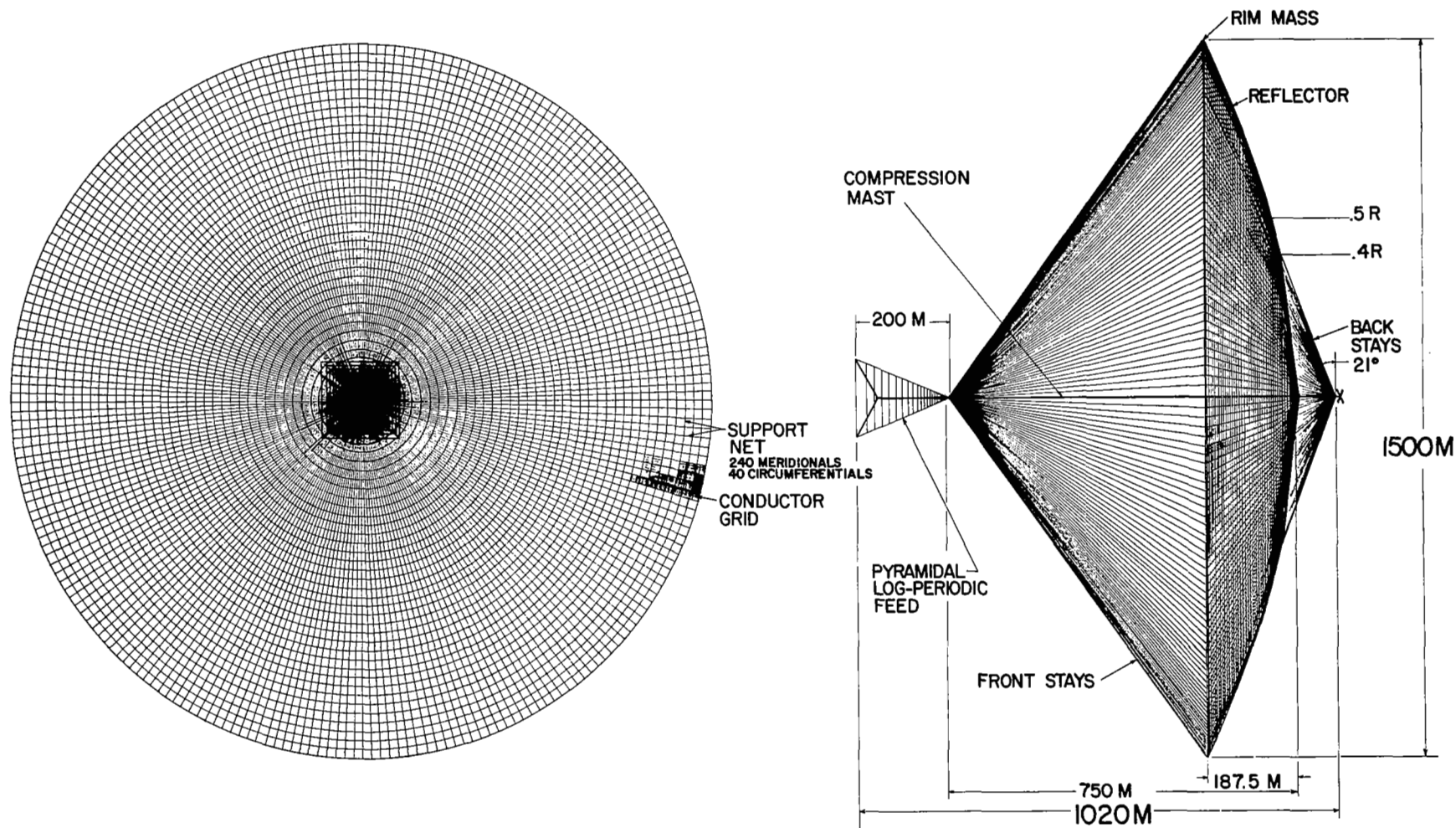
Figure 13. Near Parabolic LOFT Concept

Support Cable

Aluminized Conductor
Grid

20m

Hinged
Joint
Ring

Spot
Weld

1m

Tri-Filar Support Cable
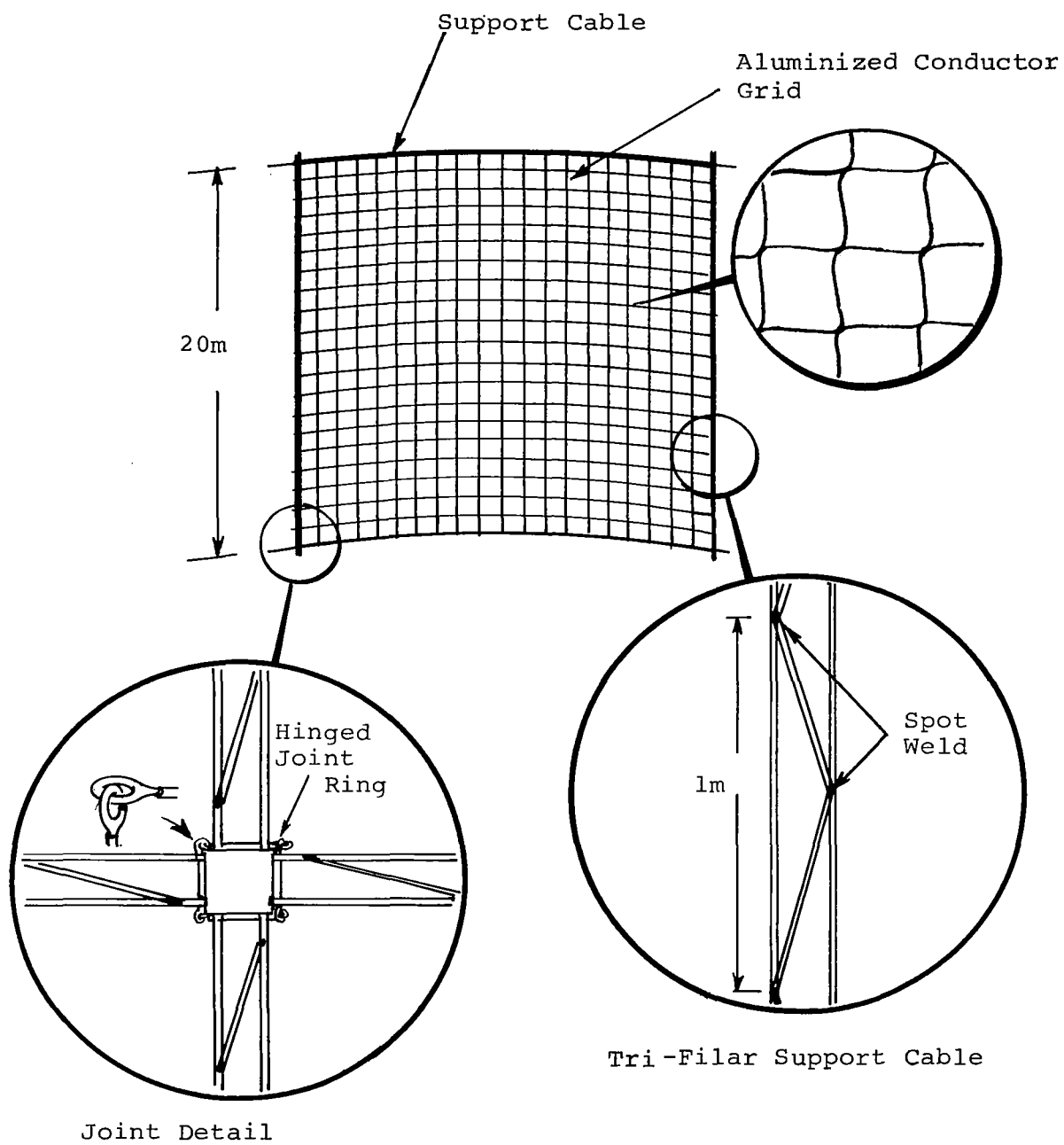
Joint Detail

Figure 14. Reflector Network Detail

37
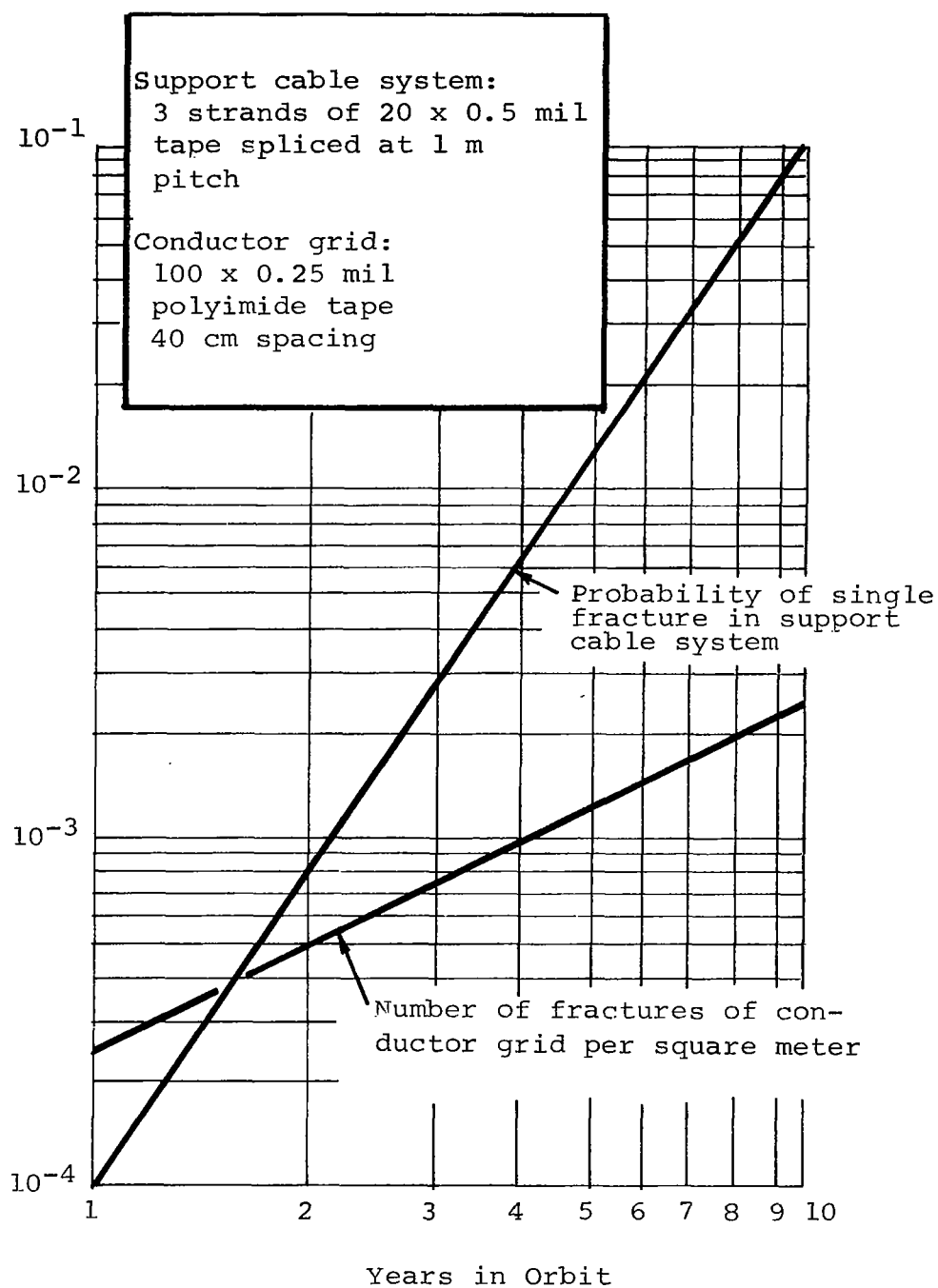
Figure 15. Micrometeoroid Fracture of Conductor
Grid and Support Cable System
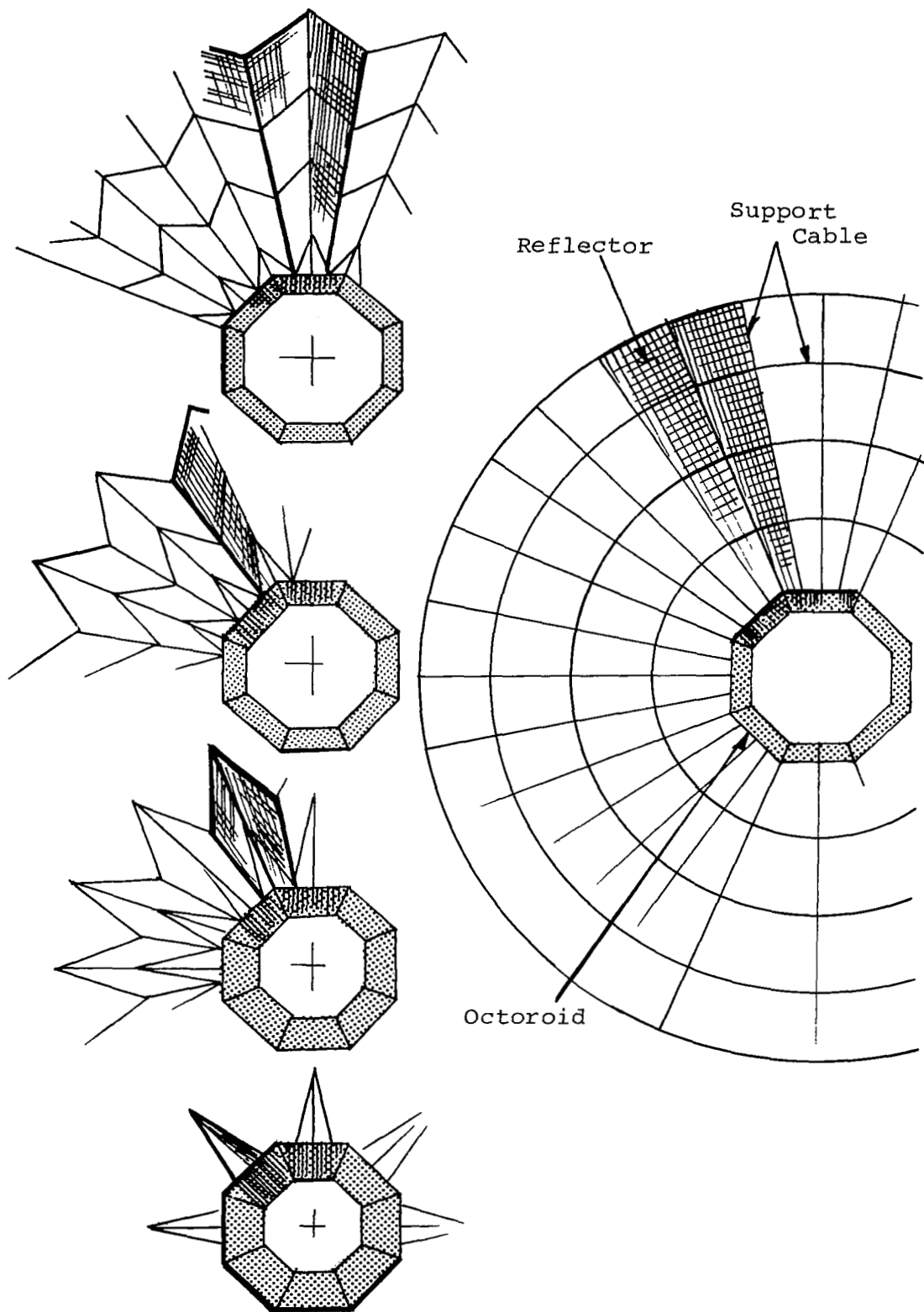
Figure 16.   Schematic Folding Concept
for Reflector Net

39

1.523 m radius

60°

2.64 m

2.59m
(typ)

760 m

2.64 m

2.59m

1.27 cm
Aluminum
Alloy
Tubing

0.508 cm wide
x 0.00254 cm thick

1.27 cm

Structural elements

Longerons: 7075 -T6 Aluminum Tubing
1.22 cm dia x 0.033 cm wall
thickness.

Battens: 7075-T6 Aluminum Tubing
1.22 cm dia. x 0.0254 cm wall
thickness.

Diagonals: 2024-T3 Aluminum Foil Strips
0.508 cm wide x 0.00254 cm thick

a) Overall LOFT
Mast

b) Section Detail

Figure 17.   Baseline Design of LOFT Mast

40

Longeron

Pivot

Teflon Washer

Diagonal
Strip

Diagonal Attach
Concept

Teflon Washer

Keeper

Batten
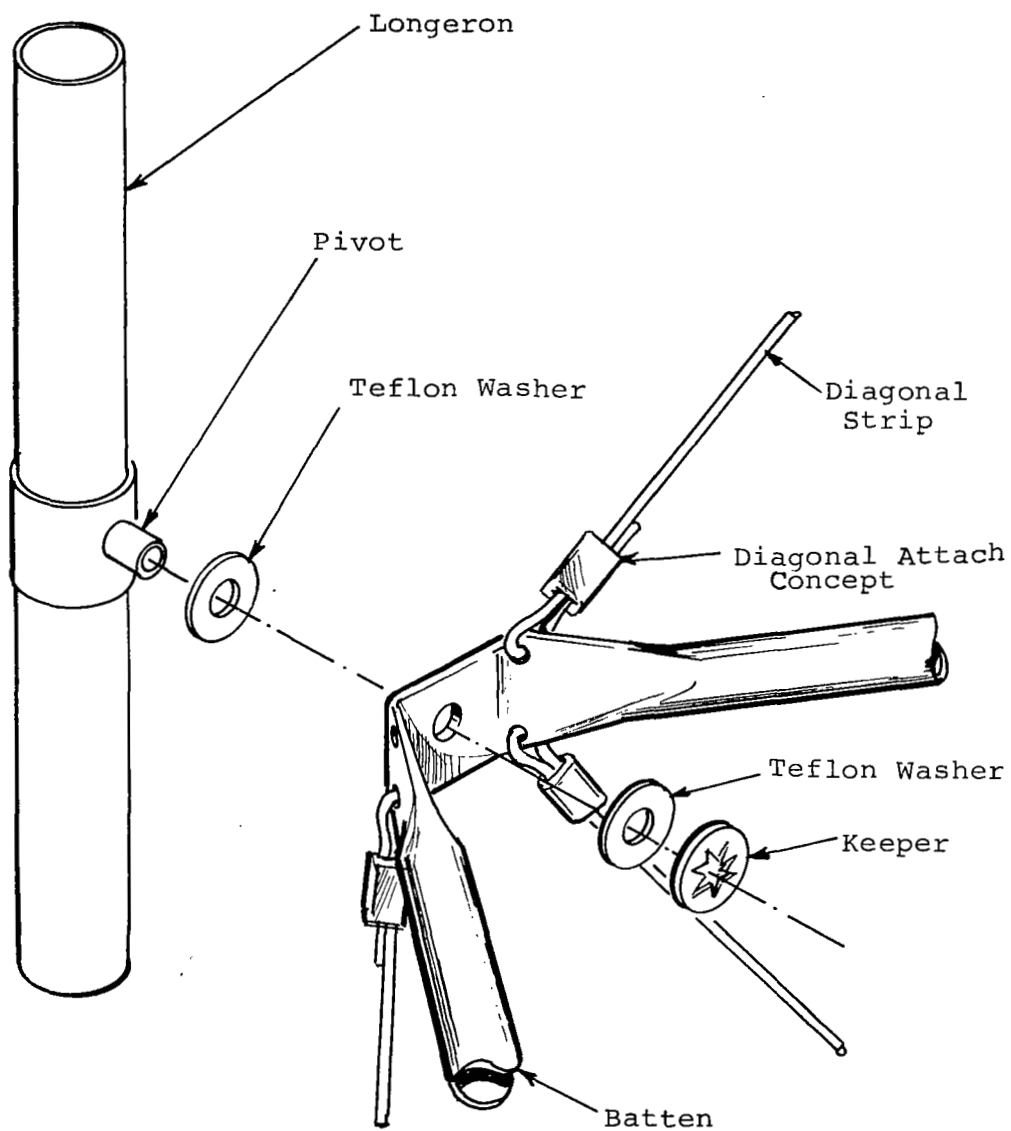
Figure 18.   LOFT Mast Joint Detail

41
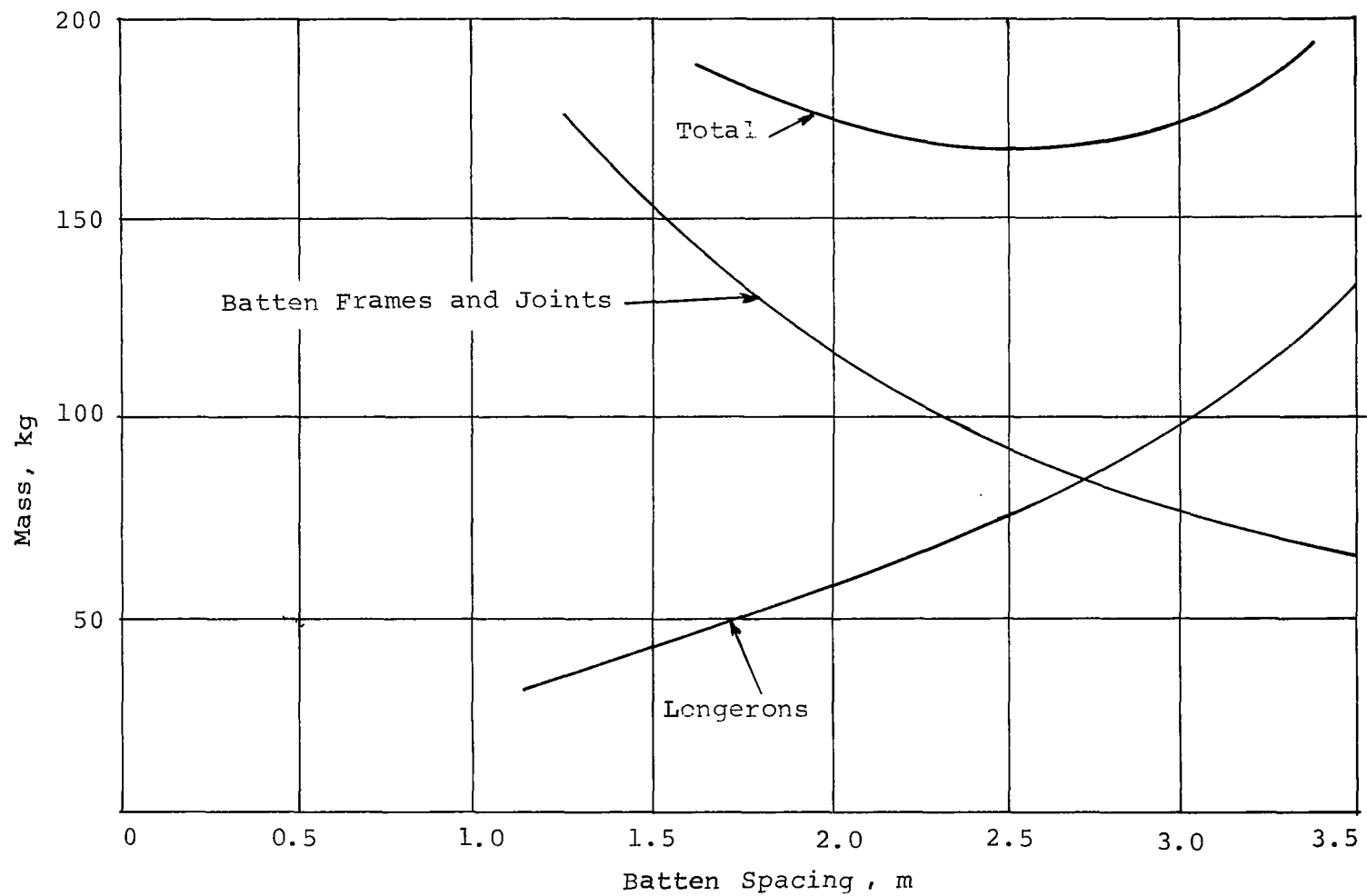
Figure 19.   Mass Tradeoff for Lattice Column Made from 0.25 mm Wall
Thickness Aluminum Alloy Tubing
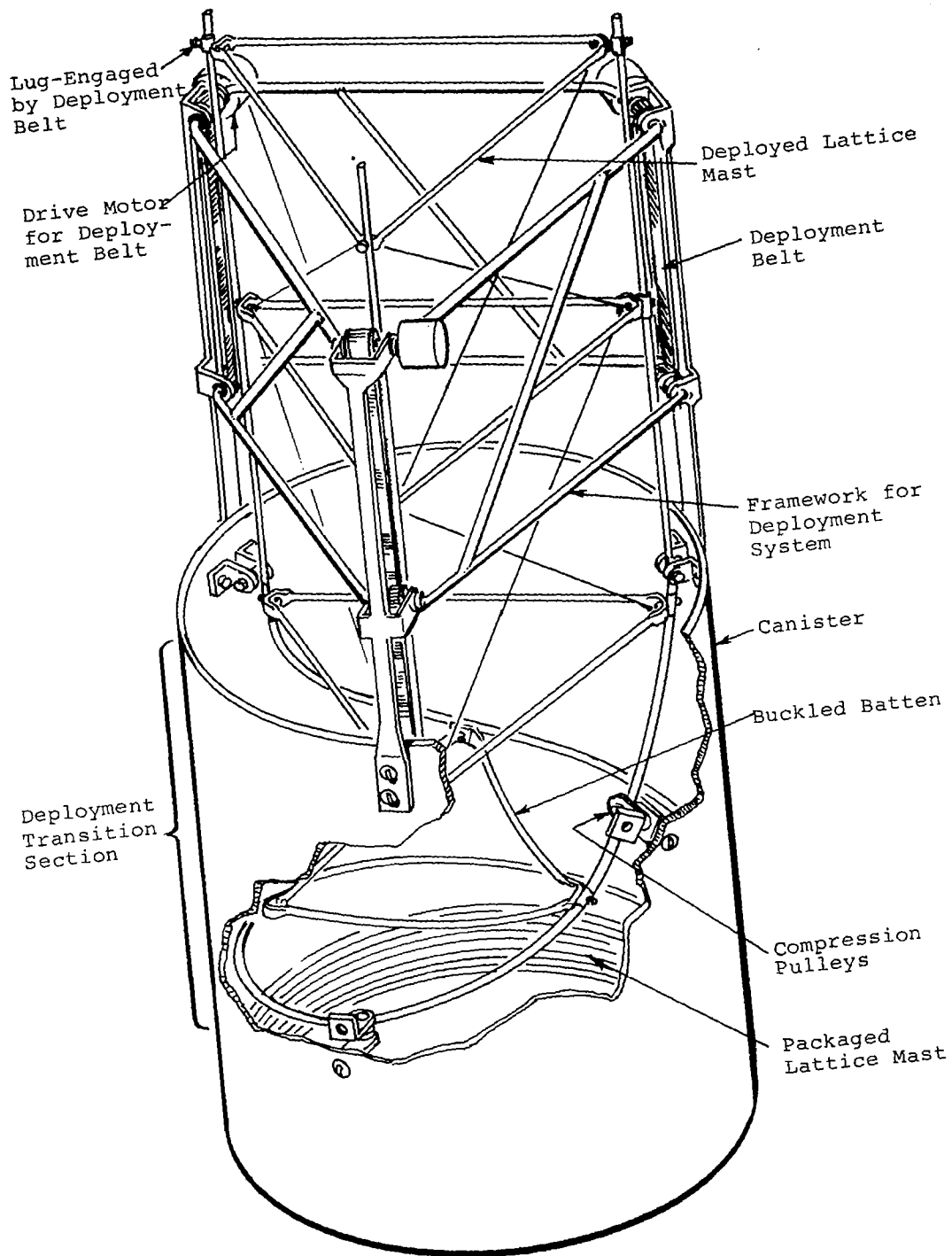
Figure 20. Deployment Mechanism for LOFT Mast

43
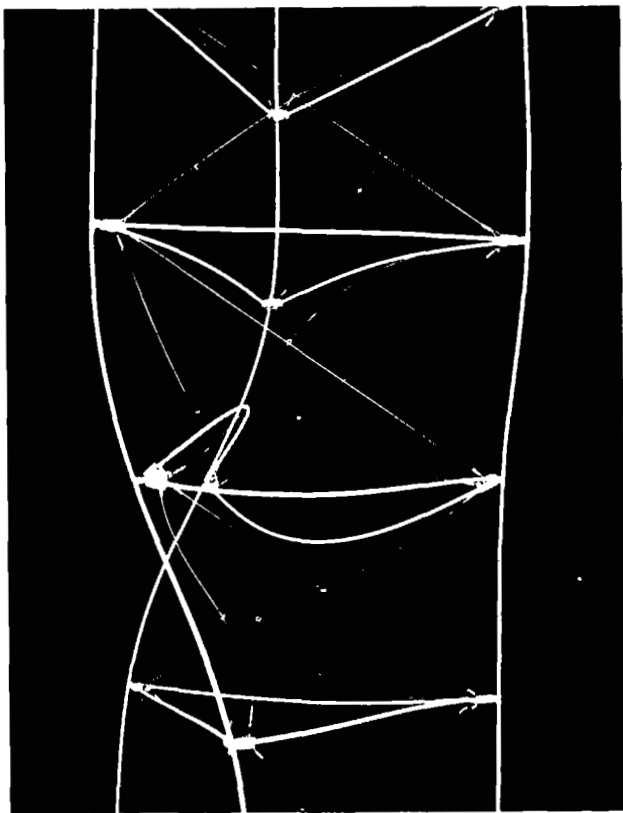
Figure   21.   Partially Deployed
                 Column
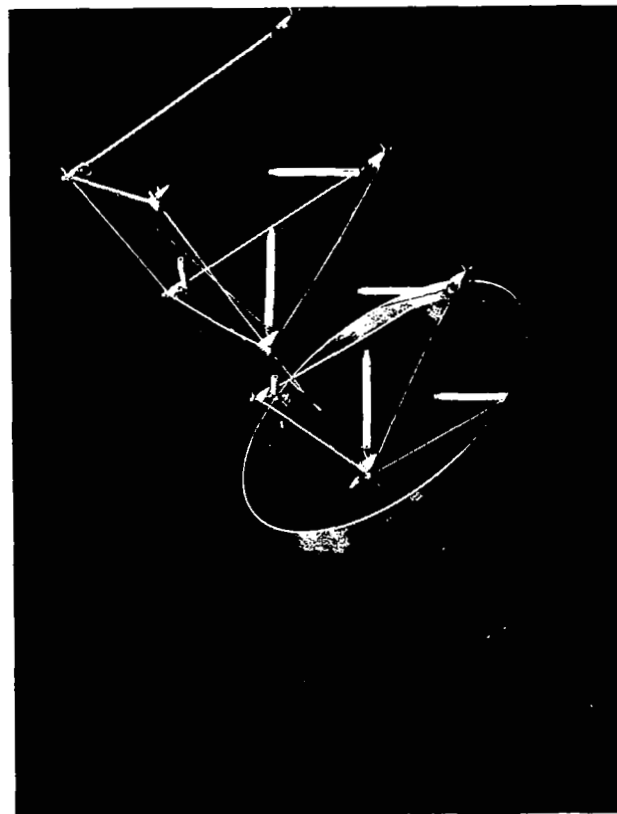
Figure   22.   Column Folding into
                 Canister

SPIN UP
ASSEMBLY

OCTOROID

BACK STAYS

FEED
PACKAGE

FRONT
BOBBINS

MAST
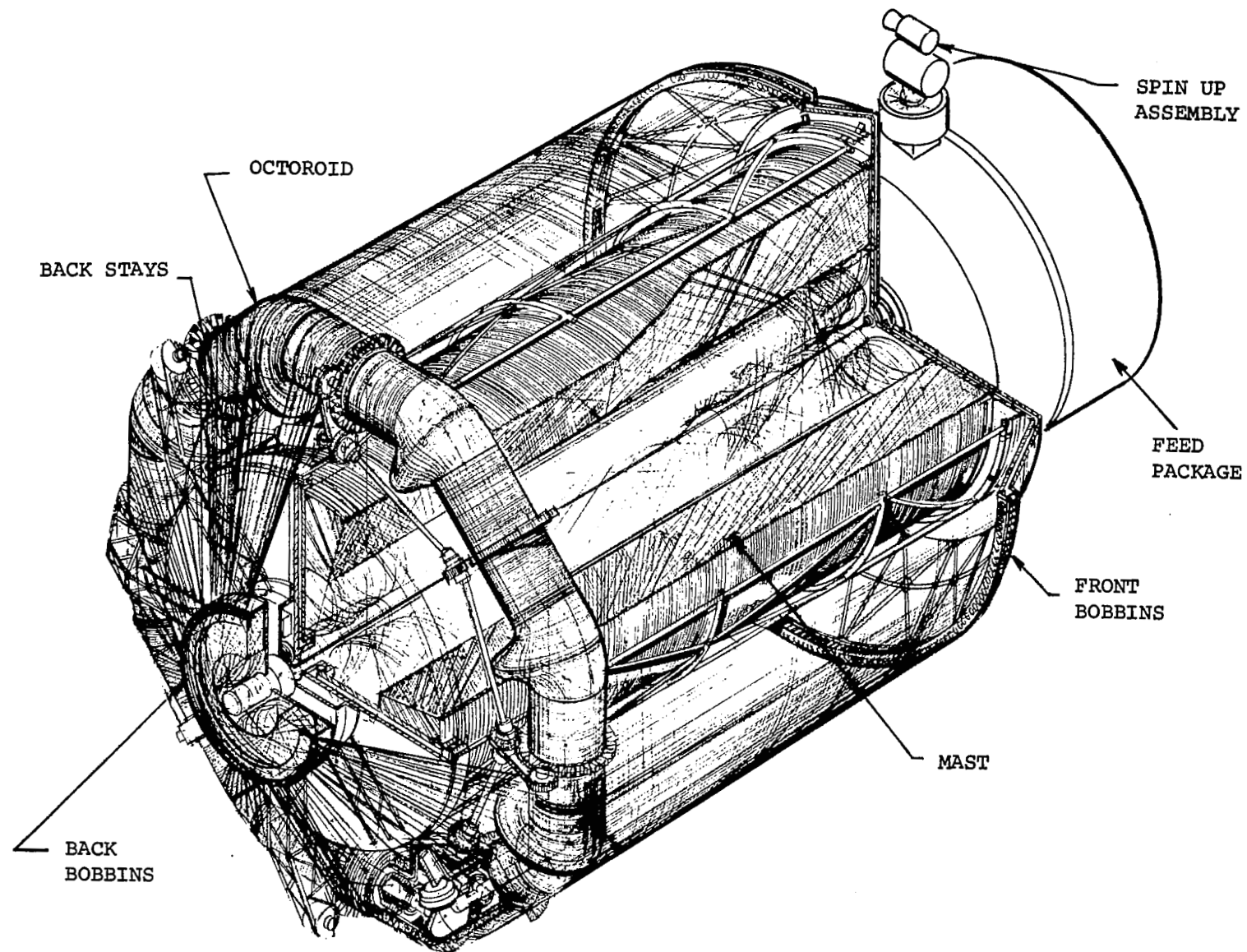
BACK
BOBBINS

Figure 23. Launch Package

BACK-STAY
BOBBINS

CONDUCTOR
GRID

COMPRESSION
MAST

FRONT-STAY
BOBBINS

BACK STAYS

BACK MAST

FRONT
STAYS

OCTOROID

RIM MASS
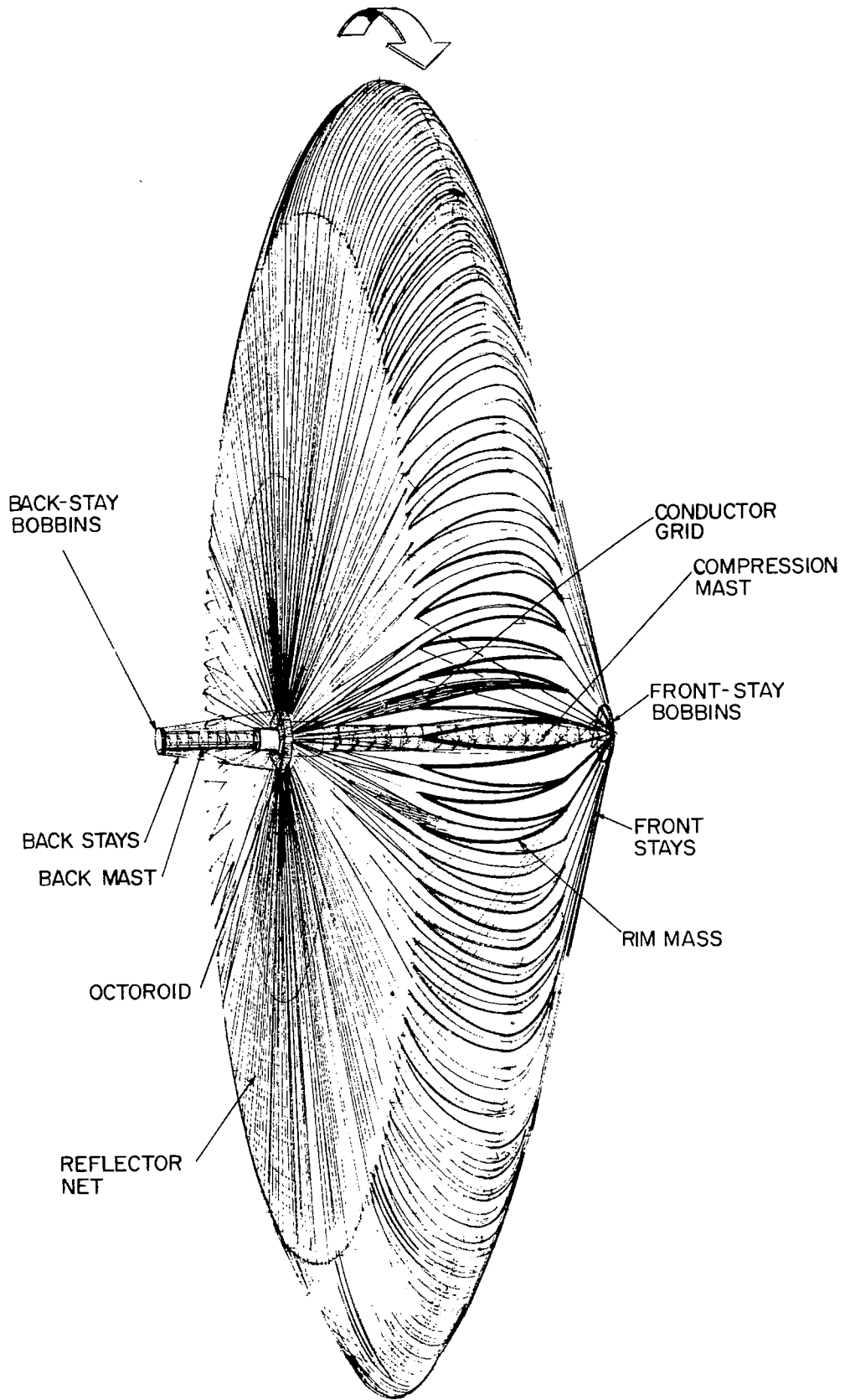
REFLECTOR
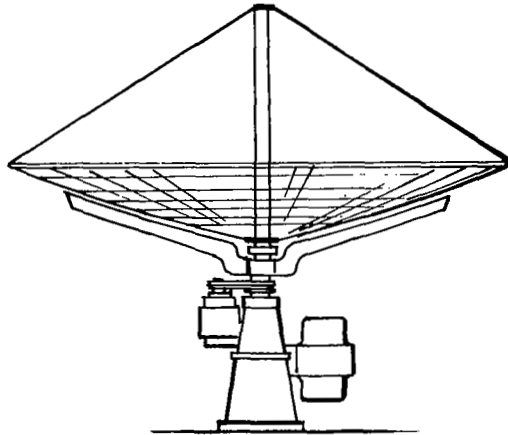NET

Figure 24.   Early Stage of Deployment
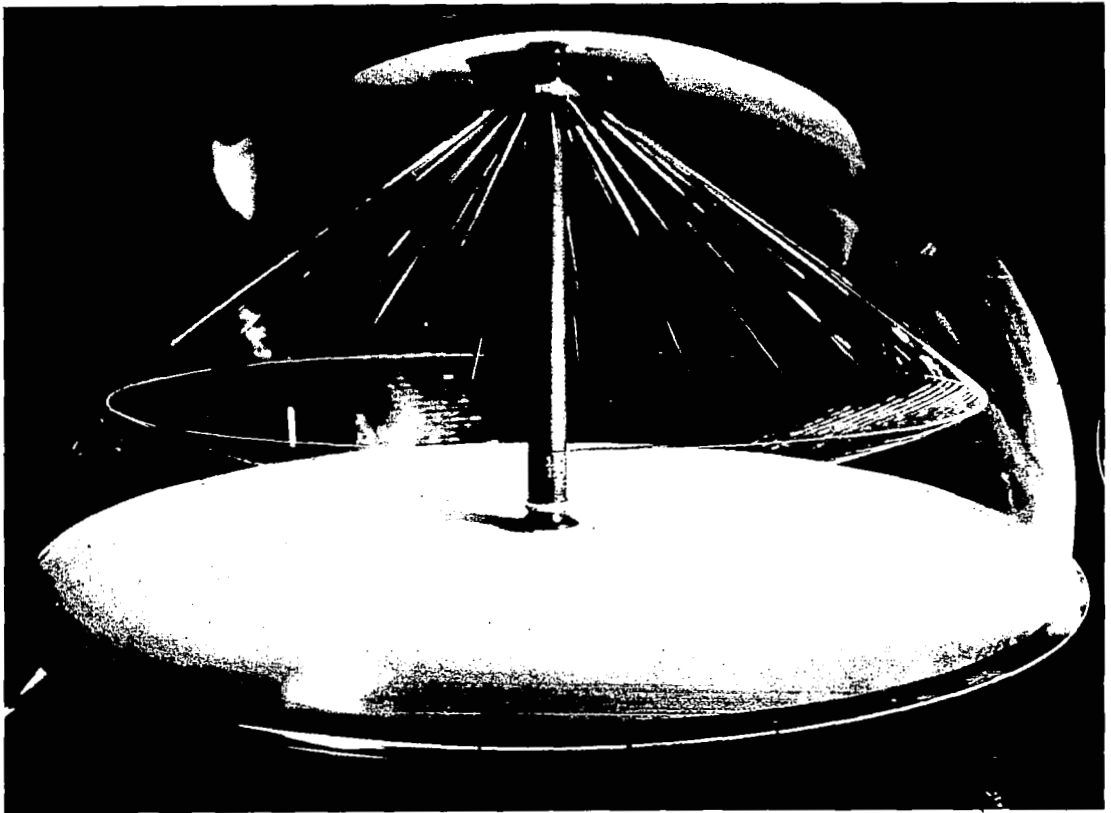
46
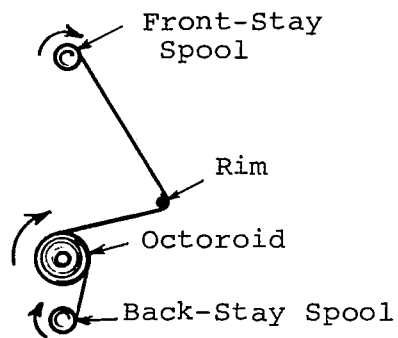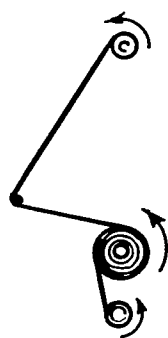
INITIAL DEPLOYMENT
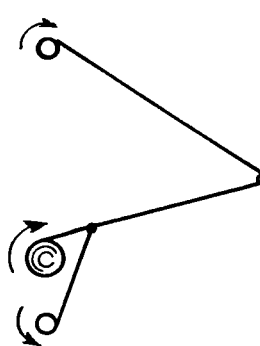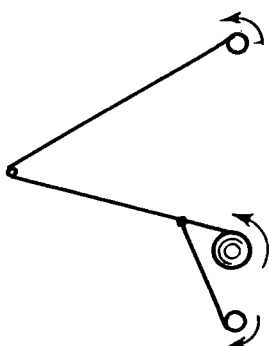
DEPLOYED 60%
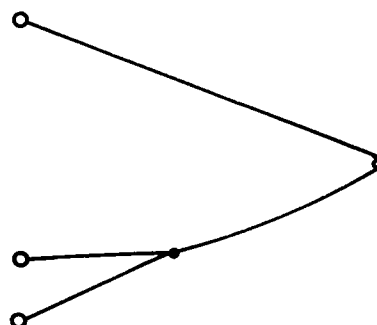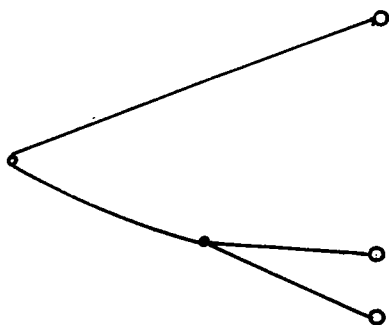
FULLY DEPLOYED

Figure 25. Schematic of Reflector, Back-Stay and Front-
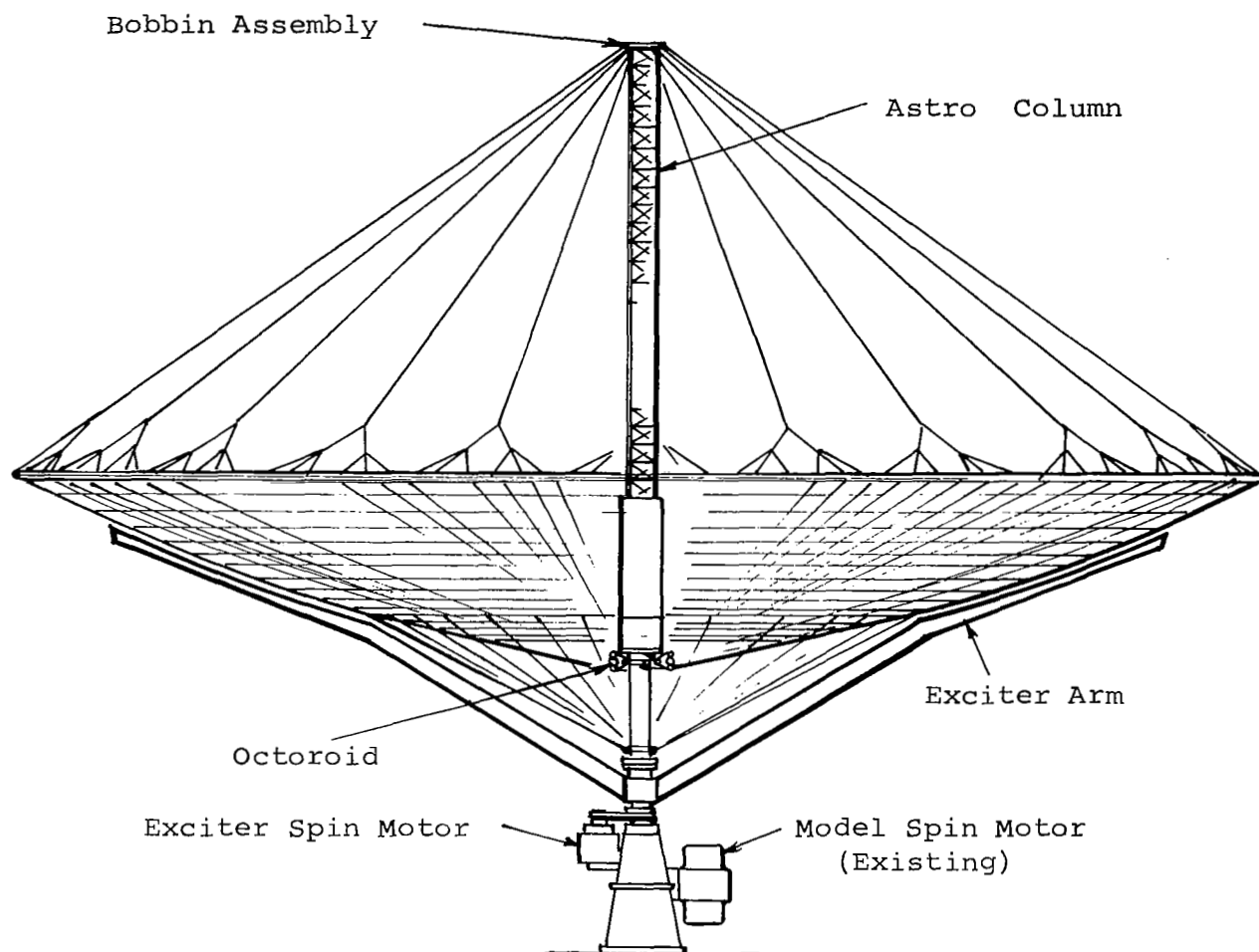Tape Reel-Out Kinematics

Schematic View

Spin Test

Figure 26.   2-Meter Model

Figure 27. Schematic View of 5-Meter Model